Title: Cell Intrinsic pH-regulated Control of Death and Proliferation of Lymphocytes in Immune Response and Tumor Cells

Wei-ping Zeng, Ph.D.[1,*]

[1]Therazwimm Corporation, 3128 Ferguson Road, Huntington, WV 25705

[*]Correspondence: Wei-ping Zeng, Therazwimm Corporation, 3128 Ferguson Road, WV 25705, USA. E-mail: weipingzengny@gmail.com.

Abstract

Cell death and proliferation are fundamental to the regulation of immune response and tumorigenesis. The present study found that low intracellular pH correlated with apoptosis of lymphocytes and tumor cells. Acid treatments lowered intracellular pH, and promoted apoptosis. Proliferating cells were more susceptible than non-proliferating cells to the low pH-induced death. In contrast, high intracellular pH correlated with cell survival. Alkaline treatments increased intracellular pH and proliferating lymphocytes, and preserved proliferating tumor cells. High mitochondrial energetic activity as measured by mitochondrial membrane potential was directly associated with low intracellular pH in lymphocytes during an active immune response. Based on these findings, the Warburg effect can be explained as necessary for proliferating cells to avoid the overuse of mitochondrial respiration for energy production, thereby maintain relatively high intracellular pH to escape from apoptosis.

Introduction

Cell death and proliferation play fundamental roles in numerous biological processes throughout the life cycle of an organism. In humans and animals, cell death and proliferation are key to understanding immune response and tumorigenesis, two biological processes that are of particular importance for the health of an individual. An immune response commences with lymphocyte clonal expansion and ends with the death of most of the expanded lymphocytes by apoptosis, in which mitochondria play critical roles [1-7]. Unlike normal lymphocytes, tumor cells are characteristically resistant to death, and can endlessly proliferate. In many tumor cells, the genes for apoptosis inhibitors are over expressed or amplified whereas genes for apoptosis activators are suppressed or deleted [8]. On the other hand, mammalian cell proliferation is primarily controlled at the "restriction point" by retinoblastoma family proteins (pRB) [9,10]. Mitogenic signals trigger a sequence of events that lead to the phosphorylation of the pRB proteins[11-14]. Phosphorylated pRB proteins dissociate from E2F family transcription factors to allow the latter to activate target gene expression, which drives the cell to pass the restriction point, transition from G1 to S phase, and commit to completing the cell cycle [15,16]. These events take place from the cell membrane to cytosol and the nucleus, but outside the mitochondria.

However, mitochondria are efficient energy producers via aerobic respiration. Given the increased demand for energy by the proliferating cells, one might expect that mitochondria positively regulate both apoptosis and proliferation. On the contrary, almost a century ago Otto Warburg observed that cell malignant transformation includes a precancerous phase, in which the cell must incur irreversible "injury of respiration" or "uncoupling of respiration and phosphorylation" and switch energy production from mitochondrial respiration to glycolysis followed by pyruvate fermentation and excretion of the fermentation waste product lactate [17,18].

This phenomenon has come to be known as the "Warburg effect", and later found in 70-80% human cancers and shared by both tumor and normal proliferating cells including lymphocytes [19-21]. More recently, studies have identified the PI3K/AKT/mTOR pathway as the mechanism for promoting Warburg effect. This pathway directly or through HIFα regulates glucose import to the cell and the expression or activities of metabolic enzymes that favor glycolysis over mitochondrial carbon oxidation (reviewed in [22,23]). Studies have also unveiled an unexpected role of energy metabolism in T cell subset differentiation. It is found that T helper effector cells preferentially use glycolysis, whereas Treg cells and memory CD8 T cells preferentially use mitochondrial respiration, to produce energy [24-31]. The mTOR has been proposed as a central integrator of immunological signals to drive the T cell differentiation [23].

Yet the cardinal feature of Warburg effect is its low efficiency of energy production as it produces only 2 ATPs per glucose as opposed to 32 ATPs through mitochondrial respiration [32]. Despite the recent progresses, why proliferating cells adopt such low-efficiency energy metabolism remains poorly understood. It could not be explained by mitochondrial injury as originally suggested by Warburg because mitochondria in most tumor cells and normal proliferating cells are not "injured" but functional [20,33]. Thus, it is even more baffling why the low energy efficient Warburg effect occurs even under normoxic and nutrient poor conditions [20]. Given the high demand for energy, it would seem more logical for proliferating cells to use mitochondrial respiration instead of Warburg effect to produce ATPs from limited fuel. One theory to explain this paradox is that Warburg effect can produce ATPs at faster speed [20]. Another theory is that Warburg effect increases glycolysis intermediate products, which can be diverted as substrates to biomass synthesis [19]. Under these theories, the Warburg effect appears to play auxiliary roles in cell proliferation but may not be indispensable.

In contrast, this article shows that low intracellular pH promotes apoptosis whereas high intracellular pH allows a cell to escape from apoptosis and proliferate at high rate. Furthermore, mitochondrial energetic activity is directly associated with low intracellular pH. Therefore, mitochondrial do in fact control both cell death and proliferation by regulating intracellular pH, and the Warburg effect can be explained as indispensable for proliferating cells to avoid excessive mitochondrial respiration hence low pH-induced death.

Results

The current study stemmed from an unexpected observation of thymic atrophy in mice that had received a test compound prepared in an acidic solution. (Manuscript in preparation). Since thymus is one of a few organs in adults that maintain active cell proliferation, this observation led to the investigation of whether pH regulates immune responses by affecting lymphocyte survival and proliferation.

Positive relationship between intracellular pH and lymphocyte proliferation

To determine whether there is a natural correlation between intracellular pH and proliferation, lymph node cells were labeled with CFSE, and cultured with either IL-2 alone or IL-2 and anti-CD3 antibodies for the study of T cell proliferation, or alternatively with either IL-4 alone or IL-4 and the B cell mitogen lipopolysaccharide (LPS) for the study of B cell proliferation. Lymphocyte proliferation was measured by the serial dilution of the CFSE signals after each cell division, whereas the intracellular pH was measured by the fluorescence intensity of the pH indicator pHrodo^{TM} Red that inversely correlates with intracellular pH. Proliferating lymphocytes were detected even in cultures with IL-2 or IL-4 alone, indicating the pre-existence of proliferating cells prior to anti-CD3 or LPS stimulation. (Fig. 1a and b). As expected, proliferating cells (CFSE^{lo}) increased with concurrent decrease of non-proliferating cells

($CFSE^{hi}$) after stimulation by anti-CD3 antibodies or LPS. Even the pre-existent proliferating cells underwent further divisions as evidenced by the decrease of their CFSE signals. (Fig. 1a and b). Importantly, the highly proliferating cells that had undergone more than 3 divisions were almost exclusively in the cell populations of high intracellular pH, whereas cells that had fewer than 3 divisions were in cell populations of low intracellular pH. (Fig. 1a and b).

Effects *of in vitro treatments with pH modifiers on proliferating lymphocytes*

To determine whether treatments with pH modifiers such as acid and base could alter the intracellular pH of lymphocytes, mediastinal lymph node (MLN) cells of mice sensitized and challenged with OVA were treated with saline or saline plus HOAc or NaOH in FBS in a 37°C water bath. Such in vitro cultures were designed to be free of interference by pH buffering agents in common tissue culture system. As compared with saline treatment, HOAc treatment lowered whereas NaOH treatment raised the intracellular pH of total lymphocytes, CD4, CD8 T cells and B cells. (suppl. Fig. 1a).

The effects of the in vitro treatment on lymphocyte proliferation were investigated by analyzing the expression of Ki-67, a widely used, dependable marker for proliferating cells whose level positively correlates with rRNA and DNA synthesis [34]. In vitro treatments with HOAc or HCl eliminated almost all Ki-67^{+} cells in total lymphocytes, CD4, CD8 T cells and B cells. In contrast, treatment with NaOH more than tripled the percentages of Ki-67^{+} cells in the total lymphocytes and CD8 T cells, and nearly tripled the percentages of Ki-67^{+} cells in the CD4 T cells and B cells. (Fig. 2).

Effects of in vivo treatments with pH modifiers on the lymphocyte populations in the MLNs

The OVA sensitization and challenge model was used to further investigate the effects of in vivo treatments with pH modifiers on lymphocyte populations in MLNs. OVA-sensitized and

challenged mice were subject to treatments with saline or saline plus HOAc, HCl or NaOH, and MLNs were harvested 7 days after the first (or 3 days after the last) of three challenges and treatments. The total numbers of MLN cells in the HOAc-treated mice were greatly reduced as compared with those in the control saline-treated mice. The numbers of total MLN cells in the HCl-treated mice were also significantly reduced but to lesser degrees. In contrast, treatment with NaOH increased the total MLN cells. (Fig. 3a). The differences in the total MLN cells were not due to differences in Treg cells because there were similar percentages of Treg cells among the different treatment groups. (Manuscript in preparation).

The total MLN lymphocytes consisted of populations of relatively small sizes and low granularities (Lym1) and populations of larger sizes and higher granularities (Lym2). The combined percentages of Lym1 and Lym2 in the total MLN cells were similar in all treatment groups. However, while the relative proportions of Lym1 and Lym2 were similar among the saline, HCl and NaOH treatment groups, the relative proportion of Lym 2 increased in the HOAc-treated mice. (Fig. 3b, upper). Lym2 consisted mostly of B lymphoblasts, (Fig. 3b, lower right), indicating that B cells were less susceptible than T cells to depletion by HOAc. Indeed, the percentages of both CD4 and CD8 T cells in Lym2 were greatly reduced in the HOAc-treated mice, whereas they were similar among the saline, HCl, and NaOH treatment groups. (Fig. 3b, lower right). Within the Lym1, the percentage of CD8 T cells in the HOAc-treated mice was only about half of that in the saline-treated mice, the percentage of CD4 T cells was also lower but to lesser extent, but the percentage of B cells was higher due to the decrease of the T cells. (Fig. 3b, lower left). This result showed again that B cells were less susceptible to depletion by HOAc than T cells. The percentages of CD4, CD8 T cells and B cells in the Lym1 of the HCl-treated mice were similar to those of the saline-treated mice. In the NaOH-treated mice, the

percentages of CD4 and CD8 T cells were slightly decreased, whereas that of B cells was accordingly increased. (Fig. 3b, lower left). Similar depletion of lymphocytes by the acids were also observed in MLNs harvested at an earlier time of 3 days after the first of two OVA challenges and 1 day after the only acid treatment (from hereon referred to as the earlier time point). (Suppl. Fig. 2a, b).

Effects of in vivo treatments with pH modifiers on lymphocyte proliferation in the MLNs

The Lym1 populations had very few Ki-67^{hi} cells, but about 70% of the cells expressed low levels of Ki-67 in all treatment groups. (Fig. 3c). However, in the MLNs harvested at the earlier time point, the percentage of Ki-67^{lo} Lym 1 cells in the HOAc treatment group was less than half of that of the saline or HCl treatment group. (Suppl. Fig. 2c). Despite the relatively high percentage of B cells in the Lym1 of the HOAc-treated mice, the percentage of Ki-67^{hi} cells in the Lym1 B cells was lower than in the saline-treated mice. The reduction, albeit smaller, was also observed in the HCl-treated mice. (Fig. 3c). Similar results were observed in MLN cells harvested at the earlier time point. (Suppl. Fig. 2c).

The Lym2 populations were more proliferative than the Lym1 populations. HOAc treatments decreased the percentages of Ki-67^{hi} Lym2 and Lym2 B cells. (Fig. 3c). Although the percentages of Ki-67^{hi} cells in Lym2 and Lym2 B cells of the HCl–treated mice were similar to those of the saline-treated mice, their Ki-67 mean fluorescence intensities were much lower than their counterparts in the saline-treated mice. (Fig. 3d). Therefore, like HOAc, HCl also negatively regulated cell proliferation. In contrast, NaOH treatments increased the percentages of Ki-67^{hi} Lym2 and Lym2 B cells. (Fig. 3c). At the earlier time point, reductions of the percentages of Ki-67^{hi} cells of Lym2 and Lym2 B cells were observed in both the HOAc- and HCl-treated mice with more reduction in the HOAc-treated mice. (Suppl. Fig. 2c).

Thus, the in vivo acid treatments showed lesser effects than in vitro treatments on depleting proliferating lymphocytes because highly proliferating cells were more susceptible to depletion than cells of low proliferative statuses, whereas in vitro acid treatments almost completely depleted both populations. The in vivo treatments also revealed that T cells were more susceptible than B cells to the depletion by acids. The differences between in vivo and in vitro treatments could be attributable to the complexity and fluidity of the in vivo environment. For example, the transportation of the pH modifiers into and out of the MLNs were dynamic processes. The actual concentrations of the pH modifiers at which the pH modifiers acted on the lymphocytes in the MLNs could be lower, and the durations of their actions shorter, than in the in vitro treatments. In addition, circulating or newly activated lymphocytes could replenish the MLNs after each acid treatment, masking the full effects of the treatments.

Correlation between low intracellular pH and lymphocyte apoptosis

Further experiments were performed to directly determine whether low intracellular pH correlates with apoptosis. In vitro staining of steady-state peripheral lymphocytes of unimmunized mice with Annexin V and 7AAD showed that about 5% of the total lymphocytes were apoptotic, and a similar percentage of early apoptotic cells (Annexin V^{hi} 7-AAD^{-}) (see [35] for the definition of early apoptotic cells); the apoptotic and early apoptotic cells were found in CD4, CD8 T cells and B cells. (Fig. 4a). Since direct measurement of intracellular pH of apoptotic (dead) cells was not possible because of their leaky cell membranes, live early apoptotic cells were analyzed as proxies of apoptosis. In all live lymphocyte populations, the early apoptotic cells were detected primarily in cells of low intracellular pH. (Fig. 4b). Apoptotic and early apoptotic cells were also detected in the MLNs of mice sensitized and challenged with OVA. (Fig. 4c). Similar to the steady-state lymphocytes, cells of low intracellular pH in the MLNs

were enriched with early apoptotic cells (Annexin V^{hi} live cells). (Fig. 4d). Although early apoptotic cells were also detected in cells of relatively high pH (in quadrant 1 of Fig. 4d), these early apoptotic cells had lower pH than their non-apoptotic counterparts (in quadrant 4) as judged by their higher MFI of the pH indicator. (Fig. 4e).

Treatments of the MLN cells with HOAc caused apoptosis in more than 70% cells, whereas there were only 1.35% and 2.43% apoptotic cells after saline or NaOH treatment, respectively. (Fig. 4f, far left panels). However, regardless of the treatments, early apoptotic cells were found primarily in the pH low populations. (Fig. 4g). Similar results were obtained with lymphocytes from in vitro cultures of stimulation with anti-CD3 antibodies or LPS, and early apoptotic cells were predominantly detected in the populations of low intracellular pH. (Suppl. Fig. 3b, d).

Relation between high mitochondrial membrane potential and low intracellular pH

Mitochondrial respiration could potentially cause net increase of protons in the cells as the result of proton leak and CO_2 production [36,37]. To experimentally investigate this possibility, mitochondrial membrane potential was analyzed as indicator of mitochondrial energetic activity in ex vivo MLN cells from OVA sensitized and challenged mice. In B cells and CD4 T cells, distinct populations of high, medium and low mitochondrial membrane potentials and different intracellular pH were identified, whereas CD8 T cells appeared to lack the low mitochondrial membrane potential population. (Fig. 5a). The majority of the cells fell into the R1 to R4 populations, in which mitochondrial membrane potential showed a prominent negative correlation with intracellular pH, and cells of low intracellular pH were found in the cells of high mitochondrial membrane potentials. (Fig. 5b). However, small numbers of cells of low intracellular pH, particularly in the CD4 T cells but also in B cells and CD8 T cells, were found

in the cells with medium and low mitochondrial potentials, which were designated as energy R.ei and R.ed populations, which likely had insufficient and deficient mitochondrial energy production, respectively. (Fig. 5a). The low intracellular pH in these cells was likely caused by excessive ATP hydrolysis instead of mitochondrial respiration. In the R1 to R4 populations, early apoptotic (Annexin V^{high}) cells were detected exclusively in the R1 populations, which had the highest mitochondrial membrane potentials and lowest intracellular pH. (Fig. 5c). Consistent with their low intracellular pH, most R.ei and R.ed cells were Annexin V^{high} early apoptotic cells. (Fig. 5d).

Effects of treatments with pH modifiers on tumor cell viability and proliferation

Cell proliferation is a common feature of immune response and tumorigenesis. To determine weather the pH modifiers would have effects on tumor cells similar to those on proliferating normal lymphocytes, the human T and B cell tumor cell lines Jurkat and Raji, respectively, were treated with saline or saline plus HOAc or NaOH in FBS. Like in the primary lymphocytes, treatment with HOAc decreased whereas treatment with NaOH increased intracellular pH. (Suppl. Fig. 1b). Compared with saline treatment, HOAc treatment greatly reduced the viabilities of the Jurkat and Raji cells as determined by Trypan Blue staining, whereas NaOH treatment only slightly decreased the viabilities. (Fig. 6a). The effects of HCl treatments on cell viability were similar to those of the HOAc treatments. (Suppl. Fig. 4). After saline treatment, the majority of live Jurkat cells remained Ki-67^{+}. However, few, if any, (<2%) live Jurkat cells after the HOAc treatment were Ki-67^{+}. In contrast, the percentage of Ki-67^{+} live Jurkat cells after NaOH treatment was similar to that after saline treatment. (Fig. 6b, upper). In Raji cells, HOAc treatment dramatically reduced the percentage of Ki-67^{hi} cells as compared with saline treatment, whereas the percentage of Ki-67^{hi} Raji cells after NaOH treatment was

similar to that after saline treatment. (Fig. 6b, lower). These results demonstrated that the proliferative statuses of the tumor cells are positively correlated with their susceptibilities to depletion by the acid treatments.

Low pH correlated with tumor cell apoptosis

Apoptotic Jurkat and Raji cells were detected in all treatment groups. (Fig. 6c and d, upper). The percentages of apoptotic cells detected in the saline and NaOH treatment groups were much higher than the percentages of dead cells determined by Trypan Blue staining in Fig. 6a. This was likely due to additional apoptotic cell death caused by the removal of the tumor cells from the FBS and incubation in serum free buffers at 37°C and room temperature during staining with the pH indicator and Annexin V. Conversely, many cells that had died earlier in the HOAc treatment groups had disintegrated during the staining processes. Nonetheless, regardless of the treatments, early apoptotic cells were enriched in cells of low intracellular pH. (Fig. 6c and d, lower). Although early apoptotic cells were also found in some pH^{hi} Jurkat cells, these pH "high" early apoptotic cells had stronger staining of the pH indicator hence lower pH than their non-apoptotic pH^{hi} counterparts. (Fig. 6c, lower).

Discussion

The present study investigated the effects of pH on the survival and proliferation of normal lymphocytes and tumor cells. It was found that low intracellular pH correlated with apoptosis, and conversely high intracellular pH correlated with cell survival. In the majority of the lymphocytes during an active immune response in the MLNs, mitochondrial energetic activity as measured by mitochondrial membrane potential was a key factor that caused low intracellular pH. Consequently, early apoptotic cells appeared in the populations with the highest mitochondrial membrane potential and lowest pH (the R1 populations), but not in cells of

relatively low mitochondrial membrane potentials and high pH (R2 to R4 populations). These findings support a theory in which excessive mitochondrial energy production leads to proton accumulation in the cells, which in turn triggers apoptosis. Since proliferating cells have high demand for energy, it is necessary for them to adopt Warburg effect to avoid overuse of mitochondrial respiration for energy hence low pH-triggered apoptosis.

While the majority pH^{lo} cells had high mitochondrial membrane potential, small numbers of pH^{lo} cells had medium or low mitochondrial membrane potentials (the R.ei and R.ed populations), therefore were insufficient or deficient in mitochondrial energy production. The low intracellular pH in these cells was likely the result of imbalance between ATP hydrolysis and synthesis, which produces and removes protons from the cells, respectively. In R.ei and R.ed cells, the equilibrium was tilted towards ATP hydrolysis, resulting in accumulation of protons in the cells. Thus, mitochondrial respiration and imbalanced ATP hydrolysis appear to be two distinct causes of low intracellular pH in lymphocytes during an active immune response.

Mitochondrial respiration or carbon oxidation can cause net increase of protons in the cells through the generation of CO_2, NADH + H^+, and $FADH_2$. For example, catabolizing 1 glucose molecule through glycolysis followed by mitochondrial carbon oxidation produces 6 CO_2, 10 (NADH + H^+) and 2 $FADH_2$. CO_2 is converted to carbonic acids in the cell by carbonic anhydrase, which produces protons [37,38]. On the other hand, NADH, as well as $FADH_2$, is fed to the electron transport chain (ETC) to create mitochondrial membrane potential and proton gradient to drive ATP synthesis. However, up to 20 to 25% of mitochondrial respiration is uncoupled from ATP synthesis, which could lead to net increases of protons in the cell that spill across the mitochondrial outer membrane to the cytosol [36,39]. Consequently, if mitochondrial respiration were to increase without restriction to meet the heightened energy demand of

proliferating cells, it would lower intracellular pH to trigger apoptosis. This explains why proliferating cells must limit energy production by mitochondrial respiration and make up the lost energy production by glycolysis in the cytosol. Glycolysis produces no CO_2 and no net NADH + H^+ and $FADH_2$, and is pH neutral once the final product lactate is exported out of the cell. Glutaminolysis could be another mechanism for proliferating cells to avoid death-triggering low intracellular pH. In glutaminolysis, glutamine is deaminated to produce ammonia and glutamate. As found in many tumor cells, glutamate is often excreted from proliferating cells [40], leaving ammonia in the cells that increases intracellular pH. Glutamate can also be further metabolized to participate in the malate-aspartate shuttle to move protons from cytosol/mitochondrial intermembrane space to the matrix by the actions of malate dehydrogenases, thereby maintains high pH in the cytosol.

The interrelationships among apoptosis, intracellular pH and energy metabolism provide a new perspective for understanding the dynamics of an immune response. At low rates of proliferation lymphocytes may only need to use mitochondrial respiration to generate energy. When the proliferation rate increases, lymphocytes would have to increase Warburg effect to avoid overuse of mitochondrial respiration that could lead to intracellular acidification and consequently apoptosis. This principle could be key to understanding not only the clonal expansion phase of an immune response, but also the culling of activated lymphocytes and transition to memory cells at the end of the immune response. Conceivably, as the signals for sustaining Warburg effect and glutaminolysis subside, lymphocytes that remain highly proliferative would be forced to overuse mitochondrial respiration to meet high demand for energy thereby become self-destructive. In contrast, lymphocytes that have lowered their proliferative propensity or developed new mechanisms to sustain adequate Warburg effect and/or

glutaminolysis would avoid the overuse of mitochondrial respiration and survive to become memory cells.

Consistent with the correlation between low intracellular pH and apoptosis, acid treatments of normal lymphocytes or tumor cells lowered intracellular pH and promoted apoptosis. These results showed a causal relationship between low intracellular pH and apoptosis. In contrast, alkaline treatments raised intracellular pH, and did not increase apoptosis as compared with saline treatments. The susceptibility to the acid-induced cell death was dependent on the cell type and the proliferative statuses of the cells. T cells were more susceptible than B cells to the acid-induced death. Highly proliferating cells were more susceptible than modestly proliferating cells, which were in turn more susceptible than non-proliferating cells. In contrast, NaOH treatments were found to increase normal proliferating lymphocytes.

From a clinical point of view, these and other data as well as the theory presented in this article can be the basis for rational design of new therapies aiming to either enhance or suppress immune and inflammatory responses. In situations such as cancers and infectious diseases where there is insufficient protective immunity, pH modifiers that increase or resist the fall of intracellular pH could be used to promote lymphocyte proliferation therefore enhance protective immunity. In other situations where overzealous immune and inflammatory responses impair normal tissue structure and functions, pH modifiers that lower or resist the rise of intracellular pH may be used to dampen the overzealous immune and inflammatory responses.

This study also sheds new lights on the role of pH in tumorigenesis. A previous study found that acidic tumor microenvironment (TME) caused by lactate excretion promotes tumor cell invasion of local tissue [41]. Therefore, acidic TME is believed to promote tumorigenesis, and

neutralizing the acidic TME by alkaline treatment is proposed as anti-tumor therapy [42]. However, according to the present study, an alternative benefit of excreting lactate for tumor cells is to prevent low intracellular pH-triggered apoptosis. Accordingly, treatments that lower the intracellular pH of tumor cells could be a new class of anti-tumor therapies. In contrast, alkaline treatment may carry an inherent risk of increasing or maintaining tumor cell proliferation, but nonetheless could benefit patients by promoting the proliferation of anti-tumor immune cells.

The Warburg effect is evolutionary conserved as similar phenomena are observed across species. For example, yeast growth accelerates as glucose concentration increases. However, when the yeast growth and glucose concentration reach critical points, the yeasts switch energy production from aerobic respiration to fermentation. This phenomenon is known as Crabtree effect [43,44]. It is conceivable that the switch is necessary for the yeasts' survival because if aerobic respiration continues to increase, it could lower intracellular pH to induce cell death. In bacteria, the Entner-Doudoroff glycolytic pathway is inefficient for energy production but counter intuitively is much more common among aerobic and facultative than anaerobic bacteria [45], suggesting that this pathway is needed to substitute for aerobic respiration for bacterial survival. Indeed, like the yeasts, bacteria switch to energetically inefficient metabolism when growth rate increases to a critical level [46]. Parasites also appear to adopt similar strategy during the stages of their life cycles in mammalian hosts [47-49]. Such evolutionary conservation suggests that pH modifiers could be used to control not only immune response and tumorigenesis but also the survival and proliferation of pathogens regardless of their abilities to resist current anti-microbial drugs.

Finally, in vivo acid or alkaline treatments were well tolerated by the animals in this study, suggesting that transient disturbance of pH homeostasis by treatments with pH modifiers could be applicable to human subjects. This notion is further supported by the facts that humans may experience transient severe acidosis without serious pathological consequences in the aftermath, for examples, during strenuous exercises and grand-mal seizures [50-52]. While simple acids and base were used as pH modifiers in this study, pH modifiers may include any other molecules that can modulate pH in or around a cell; and their preferential effects on normal or pathological cells can be explored to accentuate their postive therapeutic/preventive effects and diminute negative side effects.

Figure Legends

Fig. 1. Positive correlation between intracellular pH and lymphocyte proliferation.

(a) CFSE-labeled lymph node cells stimulated in vitro with IL-2, or IL-2 and anti-CD3 antibodies. Shown are flow cytometric pseudocolor plots of CFSE signals and intracellular pH, and histograms of CFSE signals of live total lymphocytes, CD4, CD8 T cells and B cells.

(b) CFSE-labeled lymph node cells stimulated in vitro with IL-4 or IL-4 and LPS.

Fig. 2. Effects of in vitro treatments with pH modifiers on lymphocyte proliferation. Primary lymph node cells were incubated in FBS containing 10% saline or saline plus HCl, HOAc or NaOH, then analyzed by flow cytometry to determine Ki-67 expression in live total lymphocytes, CD4, CD8 T cells and B cells ($CD19^+$). Left panels are histograms of Ki-67 expression in the different lymphocyte populations. Right panel is graphic presentation of the percentages of $Ki\text{-}67^+$ cells in the left panels.

Fig. 3. Effects of in vivo treatments with pH modifiers on the populations and proliferation of lymphocytes in MLNs.

(a) Total numbers of MLN cells. Upper: Schematic illustration of the schedules for OVA challenges and treatments of OVA-sensitized mice with saline, or saline plus HCl, HOAc or NaOH. Arrows indicate the time points for the challenges or treatments. Lower: A graph showing the average total numbers of MLN cells of mice in the different treatment groups. Statistical significance between the saline and the other groups was determined by Student t test; * $p < 0.05$, ** $p < 0.01$.

(b) Lymphocyte populations in the MLNs. The upper panels are flow cytometric plots showing the Lym1 and Lym2 lymphocyte populations in live MLN cells of the different treatment groups. The lower panels show the populations of CD4, CD8 T cells and B cells ($CD19^{+}$) in Lym1 and Lym2. Numbers in the plots are the percentages of each cell populations.

(c) Expression of Ki-67. Left panels are histograms showing Ki-67 expression, and the percentages of Ki-67 high, low, and negative cells in Lym1, Lym2 and B cells thereof. Right panels are graphic presentation of the percentages of the Ki-67 high and low cells in the left panels.

(d) Mean fluorescence intensities of Ki-67^{hi} cells in the Lym2 populations and their B cells of the different treatment groups.

Fig. 4. Relation between low intracellular pH and lymphocyte apoptosis. Total lymphocytes, CD4, CD8 T cells and B cells were analyzed by flow cytometry for the staining of Annexin V, 7AAD or Zombie-violet, and the pH indicator pHrodo™ Green.

(a, b) Steady-state peripheral lymphocytes of unimmunized mice.

(a) Plots showing the staining of Annexin V and 7AAD in the different lymphocyte populations. Apoptotic cells are Annexin V^{hi} $7AAD^{+}$, early apoptotic cells are Annexin V^{hi} $7AAD^{-}$.

(b) Plots showing the staining of the pH indicator and Annexin V in the live ($7AAD^{-}$) populations of the different lymphocytes.

(c, d, e, f, g) Ex vivo MLN cells of OVA-sensitized and challenged mice.

(c) Plots showing the staining of Annexin V and Zombie-violet of the different lymphocytes.

(d) Plots showing the staining of Annexin V and the pH indicator in the live populations (Zombie-violet $^{lo/-}$) of the different lymphocytes.

(e) Bar graphs showing the mean fluorescence intensities (MFI) of the pH indicator staining of the early apoptotic (Annexin V^{hi}) cells in quadrant 1 (Q1) and the non-apoptotic (Annexin V^{lo}) cells in quadrant 4 (Q4) in (d).

(f, g). Effects of in vitro treatments with pH modifiers on apoptosis of the MLN lymphocytes. MLN cells from mice that were sensitized and challenged with OVA were treated in vitro with saline or saline plus HOAc or NaOH in FBS.

(f) Plots showing the staining of 7AAD and Annexin V of the different lymphocytes in the different treatment groups.

(g) Plots showing the staining of the pH indicator and Annexin V in the live populations of the different lymphocytes.

Fig. 5. Relations between mitochondrial membrane potentials and intracellular pH and apoptosis. OVA sensitized mice were challenged with OVA on day 1 and 2, and MLNs were harvested on

day 3. MLN cells were stained with MitoSpy and the pH indicator. Flow cytometric analyses of live B cells, CD4 and CD8 T cells are shown.

(a) Pseudocolor plots of MitoSpy and the pH indicator, showing the energy sufficient cell populations (R1 to R4), and energy insufficient (R.ei) and energy deficient (R.ed) populations.

(b) Scatter plots showing intracellular pH (represented by the mean fluorescence intensity (MFI) of the pH indicator staining) as the function of mitochondrial membrane potential (represented by MFI of MitoSpy staining).

(c) Overlaid histograms showing Annexin V staining of the R1 to R4 populations.

(d) Overlaid histograms showing Annexin V staining of the R.ei and R.ed populations

Fig. 6. Effects of pH modifiers on the proliferation and apoptosis of tumor cells.

(a) Comparison of the average viabilities of Jurkat and Raji cells as determined by Trypan Blue staining after treatments with saline or saline plus HOAc or NaOH in FBS. Statistical significance of differences between the saline and other treatment groups was determined by Student t test, * $p < 0.05$, ** $p < 0.01$.

(b) Histograms of Ki-67 staining in live Jurkat or Raji cells after the different treatments. The numbers in the histograms are the percentages of each population defined by their levels of Ki-67 staining.

(c) Apoptosis of Jurkat cells. Upper panels show the staining of 7AAD and Annexin V of Jurkat cells after the different treatments. Lower panels show the staining of the pH indicator and Annexin V in live ($7AAD^-$) Jurkat cells after the treatments.

(d) Apoptosis of Raji cells. Upper panels show the staining of 7AAD and Annexin V of Raji cells after the different treatments. Lower panels show the staining of the pH indicator and Annexin V in live Raji cells after the treatments.

Materials and Methods

Mice

Balb/c mice were purchased from Jackson Laboratory (Bar Harbor, ME) and housed in the animal facility of Charles River Accelerator and Development Lab (CRADL) (Cambridge, MA). Animal studies were performed according to the protocols approved by the CRADL Institutional Animal Care and Use Committee.

CFSE labeling and activation of lymph node cells

Lymph node cells were washed 3 times with plain PBS. After the wash, the cells (3-5 x 10^6/ml) were incubated in 1μm Carboxyfluorescein succinimidyl ester (CFSE) (Fluka/Sigma-Aldrich, Burlington, VT) in plain PBS at room temperature for 7 minutes. After the incubation, 1/4 volume of FBS was added to stop the labeling, and cells were washed 4 times with PBS plus 1% FBS. The labeled cells were cultured with IL-2 (20 units/ml) or IL-2 plus anti-CD3 antibody (1μg/ml) (BD Pharmingen (San Diego, CA). Alternatively, the labeled cells were cultured with IL-4 (4ng/ml) or IL-4 plus lipopolysaccharide (LPS) (10μg/ml) (Sigma-Aldrich, St. Louis, MO). Two and half days later, cells were harvested for further experiments.

Measuring intracellular pH and mitochondrial membrane potential

The intracellular pH indicators pHrodo™ Green/Red AM were purchased from ThermoFisher Scientific (Waltham, MA), and MitoSpy Orange was purchased from Biolegend (San Francisco, CA). Cells were washed once with Live Cell Image Solution (LCIS) (Life Technoology/ThermoFisher Scientific, Grand Island, NY). Immediately prior to use, the pH indicator pHrodo™ Greenn/Red AM and the PowerLoad were mixed then diluted in the LCIS to produce working solution containing 0.5-1μM pH indicator and/or 100nM MitoSpy Orange. The cells (1-2 x 10^7/ml) were suspended in the working solution and incubated in a 37°C water bath for 30 minutes. After the incubation, the cells were washed once in LCIS containing 1% FBS. The levels of staining were analyzed by flow cytometry.

OVA sensitization, challenge and treatments of mice

OVA sensitization and challenge were performed as previously described. [53,54]. Briefly, Balb/c mice were sensitized by i.p. injection of 20μg OVA (Sigma-Aldrich, St. Louis, MO) plus Alum adjuvant (Thermo Scientific, Rockford, IL). Two weeks later, the sensitization is repeated with 500μg OVA. About two weeks later, mice were challenged with 100μg OVA in 60μl saline by intratracheal (i.t.) instillation, and the challenges were repeated as described in each experiment. For treatments, mice received i.t. instillation of 60μl saline or saline containing 175mM HOAc or HCl along with OVA challenge. Since mice were less tolerant to i.t. instillation of NaOH, NaOH treatments were carried out by i.p. injection of 200μl of saline containing 87.5mM NaOH. After the challenges and treatments, mediastinal lymph nodes were collected at the times specified in the different experiments.

In vitro treatments of lymphocytes and tumor cells

Lymph node cells (4 x 10^6 cells/ml) were incubated in FBS containing 10% of saline or saline plus 87.5mM HCl, HOAc or NaOH in 37°C water bath for 5 hours before analyses. The

Jurkat and Raji cells (2 x 10^6 cells/ml) were incubated in FBS containing 10% saline or 87.5mM HCl, HOAc or NaOH prepared in saline in 37°C water bath for 3-5 hours. For measuring the alteration of intracellular pH, cells stained with pHrodo^{TM} Green were treated for 20 min.

Flow cytometry

Fluorochrome-conjugated antibodies against mouse CD3, CD4, CD8, CD19 and Ki-67, and against human Ki-67, Zombie-Green/Violet fixable viability dyes and Foxp3 buffer set were purchased from Biolegend (San Diego, CA). Lymphocytes were stained for cell surface markers. Live and dead cells were distinguished by staining the cells with Zombie dyes or 7-AAD. For Ki-67 staining, cells were fixed with CytoFix/CytoPerm buffer, washed with PBS plus 1% FBS and 1x CytoPerm buffer, and incubated with antibodies against mouse or human Ki-67. Jurkat and Raji cells were stained with Zombie-Green dye followed by fixation, permealization and staining with anti-human Ki-67. (Biolegend, San Diego, CA). For Annexin V staining, cells were washed twice with plain PBS and once with Annexin V binging buffer (10mM HEPES, pH7.4, 140mM NaCl, 2.5mM $CaCl_2$) and incubated with fluorochrome-conjugated Annexin V (Biolegend) in Annexin V binding buffer for 15min at room temperature. The cells were washed twice in Annexin V binding buffer, and re-suspended in Annexin V binding buffer. 7-AAD was added to the cells before analyzed by flow cytometry to distinguish dead and live cells.

References

1 Adachi, M., Watanabe-Fukunaga, R. & Nagata, S. Aberrant transcription caused by the insertion of an early transposable element in an intron of the Fas antigen gene of lpr mice. *Proc Natl Acad Sci U S A* **90**, 1756-1760, doi:10.1073/pnas.90.5.1756 (1993).

2 Burnet, F. *The Clonal Selection Theory of Acquired Immunity*. (Cambridge University Press, 1959).

3 Hildeman, D. A., Zhu, Y., Mitchell, T. C., Kappler, J. & Marrack, P. Molecular mechanisms of activated T cell death in vivo. *Curr Opin Immunol* **14**, 354-359, doi:10.1016/s0952-7915(02)00335-7 (2002).

4 Liu, X., Kim, C. N., Yang, J., Jemmerson, R. & Wang, X. Induction of apoptotic program in cell-free extracts: requirement for dATP and cytochrome c. *Cell* **86**, 147-157, doi:10.1016/s0092-8674(00)80085-9 (1996).

5 Jost, P. J. *et al.* XIAP discriminates between type I and type II FAS-induced apoptosis. *Nature* **460**, 1035-1039, doi:10.1038/nature08229 (2009).

6 Li, H., Zhu, H., Xu, C. J. & Yuan, J. Cleavage of BID by caspase 8 mediates the mitochondrial damage in the Fas pathway of apoptosis. *Cell* **94**, 491-501, doi:10.1016/s0092-8674(00)81590-1 (1998).

7 Luo, X., Budihardjo, I., Zou, H., Slaughter, C. & Wang, X. Bid, a Bcl2 interacting protein, mediates cytochrome c release from mitochondria in response to activation of cell surface death receptors. *Cell* **94**, 481-490, doi:10.1016/s0092-8674(00)81589-5 (1998).

8 Czabotar, P. E., Lessene, G., Strasser, A. & Adams, J. M. Control of apoptosis by the BCL-2 protein family: implications for physiology and therapy. *Nat Rev Mol Cell Biol* **15**, 49-63, doi:10.1038/nrm3722 (2014).

9 Friend, S. H. *et al.* A human DNA segment with properties of the gene that predisposes to retinoblastoma and osteosarcoma. *Nature* **323**, 643-646, doi:10.1038/323643a0 (1986).

10 Weinberg, R. A. The retinoblastoma protein and cell cycle control. *Cell* **81**, 323-330, doi:10.1016/0092-8674(95)90385-2 (1995).

11 Akiyama, T., Ohuchi, T., Sumida, S., Matsumoto, K. & Toyoshima, K. Phosphorylation of the retinoblastoma protein by cdk2. *Proc Natl Acad Sci U S A* **89**, 7900-7904, doi:10.1073/pnas.89.17.7900 (1992).

12 Ewen, M. E. *et al.* Functional interactions of the retinoblastoma protein with mammalian D-type cyclins. *Cell* **73**, 487-497, doi:10.1016/0092-8674(93)90136-e (1993).

13 Hinds, P. W. *et al.* Regulation of retinoblastoma protein functions by ectopic expression of human cyclins. *Cell* **70**, 993-1006, doi:10.1016/0092-8674(92)90249-c (1992).

14 Kato, J., Matsushime, H., Hiebert, S. W., Ewen, M. E. & Sherr, C. J. Direct binding of cyclin D to the retinoblastoma gene product (pRb) and pRb phosphorylation by the cyclin D-dependent kinase CDK4. *Genes Dev* **7**, 331-342, doi:10.1101/gad.7.3.331 (1993).

15 Chellappan, S. P., Hiebert, S., Mudryj, M., Horowitz, J. M. & Nevins, J. R. The E2F transcription factor is a cellular target for the RB protein. *Cell* **65**, 1053-1061, doi:10.1016/0092-8674(91)90557-f (1991).

16 Dyson, N. *et al.* Analysis of p107-associated proteins: p107 associates with a form of E2F that differs from pRB-associated E2F-1. *J Virol* **67**, 7641-7647, doi:10.1128/JVI.67.12.7641-7647.1993 (1993).

17 Warburg, O. Versuche an überlebendem Carcinomgewebe. *Biochem Zschr* **142**, 317–333 (1923).

18 Warburg, O. On the origin of cancer cells. *Science* **123**, 309-314, doi:10.1126/science.123.3191.309 (1956).

19 Duvel, K. *et al.* Activation of a metabolic gene regulatory network downstream of mTOR complex 1. *Mol Cell* **39**, 171-183, doi:10.1016/j.molcel.2010.06.022 (2010).

20 Vaupel, P. & Multhoff, G. The Warburg Effect: Historical Dogma Versus Current Rationale. *Adv Exp Med Biol* **1269**, 169-177, doi:10.1007/978-3-030-48238-1_27 (2021).

21 Wang, T., Marquardt, C. & Foker, J. Aerobic glycolysis during lymphocyte proliferation. *Nature* **261**, 702-705, doi:10.1038/261702a0 (1976).

22 Saxton, R. A. & Sabatini, D. M. mTOR Signaling in Growth, Metabolism, and Disease. *Cell* **168**, 960-976, doi:10.1016/j.cell.2017.02.004 (2017).

23 Waickman, A. T. & Powell, J. D. mTOR, metabolism, and the regulation of T-cell differentiation and function. *Immunol Rev* **249**, 43-58, doi:10.1111/j.1600-065X.2012.01152.x (2012).

24 Araki, K. *et al.* mTOR regulates memory CD8 T-cell differentiation. *Nature* **460**, 108-112, doi:10.1038/nature08155 (2009).

25 Delgoffe, G. M. *et al.* The mTOR kinase differentially regulates effector and regulatory T cell lineage commitment. *Immunity* **30**, 832-844, doi:10.1016/j.immuni.2009.04.014 (2009).

26 Lee, K. *et al.* Mammalian target of rapamycin protein complex 2 regulates differentiation of Th1 and Th2 cell subsets via distinct signaling pathways. *Immunity* **32**, 743-753, doi:10.1016/j.immuni.2010.06.002 (2010).

27 Michalek, R. D. *et al.* Cutting edge: distinct glycolytic and lipid oxidative metabolic programs are essential for effector and regulatory CD4+ T cell subsets. *J Immunol* **186**, 3299-3303, doi:10.4049/jimmunol.1003613 (2011).

28 Pearce, E. L. *et al.* Enhancing CD8 T-cell memory by modulating fatty acid metabolism. *Nature* **460**, 103-107, doi:10.1038/nature08097 (2009).

29 Shi, L. Z. *et al.* HIF1alpha-dependent glycolytic pathway orchestrates a metabolic checkpoint for the differentiation of TH17 and Treg cells. *J Exp Med* **208**, 1367-1376, doi:10.1084/jem.20110278 (2011).

30 Wang, R. *et al.* The transcription factor Myc controls metabolic reprogramming upon T lymphocyte activation. *Immunity* **35**, 871-882, doi:10.1016/j.immuni.2011.09.021 (2011).

31 Xu, K. *et al.* Glycolysis fuels phosphoinositide 3-kinase signaling to bolster T cell immunity. *Science* **371**, 405-410, doi:10.1126/science.abb2683 (2021).

32 Mookerjee, S. A., Gerencser, A. A., Nicholls, D. G. & Brand, M. D. Quantifying intracellular rates of glycolytic and oxidative ATP production and consumption using extracellular flux measurements. *J Biol Chem* **292**, 7189-7207, doi:10.1074/jbc.M116.774471 (2017).

33 Potter, M., Newport, E. & Morten, K. J. The Warburg effect: 80 years on. *Biochem Soc Trans* **44**, 1499-1505, doi:10.1042/BST20160094 (2016).

34 Darzynkiewicz, Z. *et al.* Initiation and termination of DNA replication during S phase in relation to cyclins D1, E and A, p21WAF1, Cdt1 and the p12 subunit of DNA polymerase delta revealed in individual cells by cytometry. *Oncotarget* **6**, 11735-11750, doi:10.18632/oncotarget.4149 (2015).

35 Vermes, I., Haanen, C., Steffens-Nakken, H. & Reutelingsperger, C. A novel assay for apoptosis. Flow cytometric detection of phosphatidylserine expression on early apoptotic cells using fluorescein labelled Annexin V. *J Immunol Methods* **184**, 39-51, doi:10.1016/0022-1759(95)00072-i (1995).

36 Rolfe, D. F. & Brown, G. C. Cellular energy utilization and molecular origin of standard metabolic rate in mammals. *Physiol Rev* **77**, 731-758, doi:10.1152/physrev.1997.77.3.731 (1997).

37 Tripp, B. C., Smith, K. & Ferry, J. G. Carbonic anhydrase: new insights for an ancient enzyme. *J Biol Chem* **276**, 48615-48618, doi:10.1074/jbc.R100045200 (2001).

38 Meldrum, N. U. & Roughton, F. J. Carbonic anhydrase. Its preparation and properties. *J Physiol* **80**, 113-142, doi:10.1113/jphysiol.1933.sp003077 (1933).

39 Fantin, V. R., St-Pierre, J. & Leder, P. Attenuation of LDH-A expression uncovers a link between glycolysis, mitochondrial physiology, and tumor maintenance. *Cancer Cell* **9**, 425-434, doi:10.1016/j.ccr.2006.04.023 (2006).

40 LeBoeuf, S. E. *et al.* Activation of Oxidative Stress Response in Cancer Generates a Druggable Dependency on Exogenous Non-essential Amino Acids. *Cell Metab* **31**, 339-350 e334, doi:10.1016/j.cmet.2019.11.012 (2020).

41 Estrella, V. *et al.* Acidity generated by the tumor microenvironment drives local invasion. *Cancer Res* **73**, 1524-1535, doi:10.1158/0008-5472.CAN-12-2796 (2013).

42 Corbet, C. & Feron, O. Tumour acidosis: from the passenger to the driver's seat. *Nat Rev Cancer* **17**, 577-593, doi:10.1038/nrc.2017.77 (2017).

43 Pfeiffer, T. & Morley, A. An evolutionary perspective on the Crabtree effect. *Front Mol Biosci* **1**, 17, doi:10.3389/fmolb.2014.00017 (2014).

44 Ziv, N., Brandt, N. J. & Gresham, D. The use of chemostats in microbial systems biology. *J Vis Exp*, doi:10.3791/50168 (2013).

45 Flamholz, A., Noor, E., Bar-Even, A., Liebermeister, W. & Milo, R. Glycolytic strategy as a tradeoff between energy yield and protein cost. *Proc Natl Acad Sci U S A* **110**, 10039-10044, doi:10.1073/pnas.1215283110 (2013).

46 Vemuri, G. N., Altman, E., Sangurdekar, D. P., Khodursky, A. B. & Eiteman, M. A. Overflow metabolism in Escherichia coli during steady-state growth: transcriptional regulation and effect of the redox ratio. *Appl Environ Microbiol* **72**, 3653-3661, doi:10.1128/AEM.72.5.3653-3661.2006 (2006).

47 Homewood, C. A. Carbohydrate metabolism of malarial parasites. *Bull World Health Organ* **55**, 229-235 (1977).

48 Moyersoen, J., Choe, J., Fan, E., Hol, W. G. & Michels, P. A. Biogenesis of peroxisomes and glycosomes: trypanosomatid glycosome assembly is a promising new drug target. *FEMS Microbiol Rev* **28**, 603-643, doi:10.1016/j.femsre.2004.06.004 (2004).

49 You, H., Stephenson, R. J., Gobert, G. N. & McManus, D. P. Revisiting glucose uptake and metabolism in schistosomes: new molecular insights for improved schistosomiasis therapies. *Front Genet* **5**, 176, doi:10.3389/fgene.2014.00176 (2014).

50 Bangsbo, J., Johansen, L., Graham, T. & Saltin, B. Lactate and H+ effluxes from human skeletal muscles during intense, dynamic exercise. *J Physiol* **462**, 115-133, doi:10.1113/jphysiol.1993.sp019546 (1993).

51 Hopkins, E. & Sharma, S. in *Physiology* (StatPearls Publishing, 2019).

52 Orringer, C. E., Eustace, J. C., Wunsch, C. D. & Gardner, L. B. Natural history of lactic acidosis after grand-mal seizures. A model for the study of an anion-gap acidosis not associated with hyperkalemia. *N Engl J Med* **297**, 796-799, doi:10.1056/NEJM197710132971502 (1977).

53 Rangasamy, T. *et al.* Disruption of Nrf2 enhances susceptibility to severe airway inflammation and asthma in mice. *J Exp Med* **202**, 47-59, doi:10.1084/jem.20050538 (2005).

54 Zeng, W. P. *et al.* Staphylococcal enterotoxin A-activated regulatory T cells promote allergen-specific TH2 response to intratracheal allergen inoculation. *J Allergy Clin Immunol* **139**, 508-518 e504, doi:10.1016/j.jaci.2016.04.033 (2017).

Acknowledgments

WZ thanks Dr. Tiru Rangasamy for technical information regarding sensitization and challenge of mice with OVA**.**

Author Contribution

WZ conceived, designed and carried out the study, and wrote the manuscript.

Competing interest

WZ is the inventor of a patent application based in part on some data presented in this article.

Data and materials availability

All data are available in the manuscript.

Figures and Legends

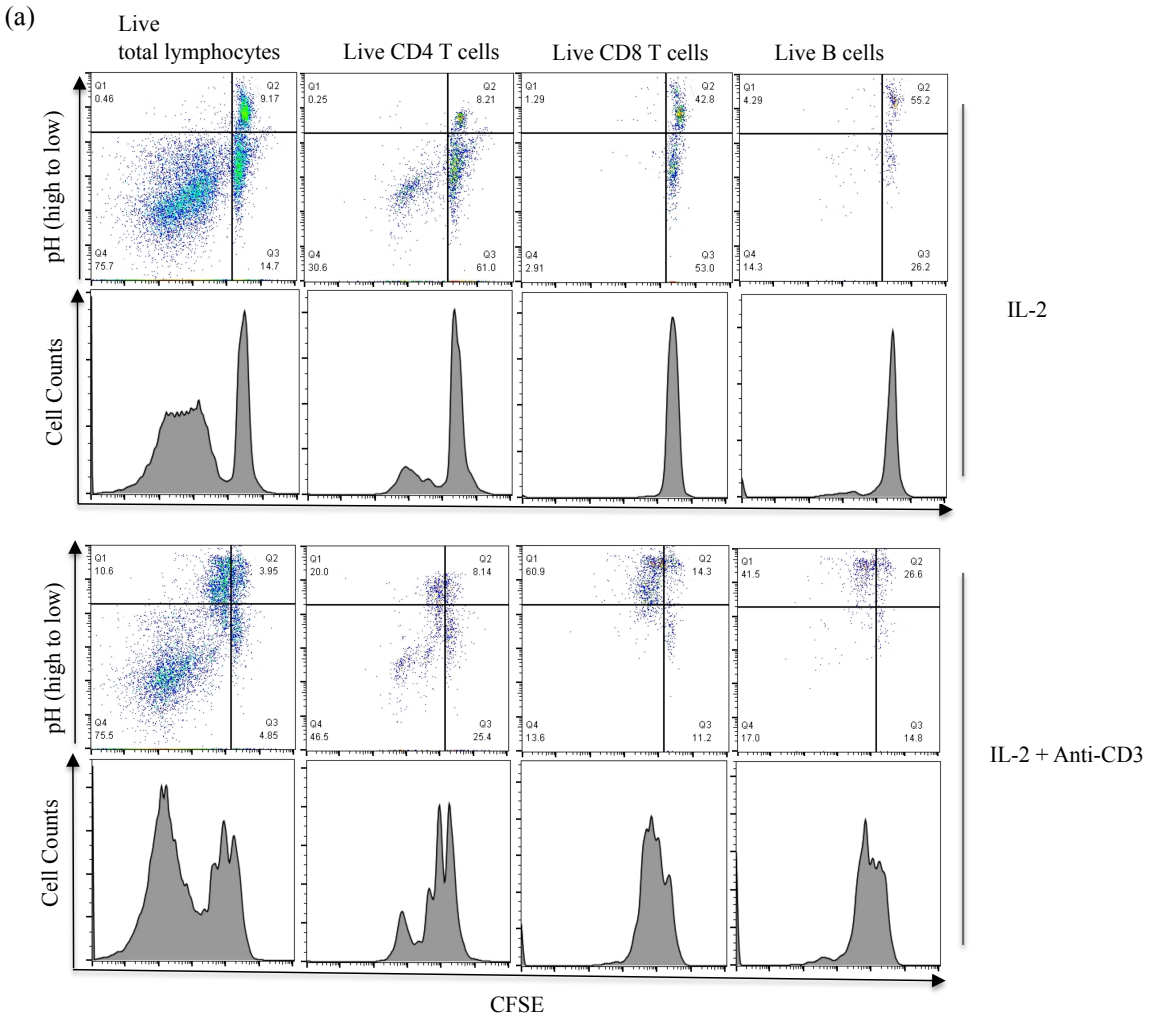

Fig. 1. Positive correlation between intracellular pH and lymphocyte proliferation.

(a) CFSE-labeled lymph node cells stimulated in vitro with IL-2, or IL-2 and anti-CD3 antibodies. Shown are flow cytometric pseudocolor plots of CFSE signals and intracellular pH, and histograms of CFSE signals of live total lymphocytes, CD4, CD8 T cells and B cells.

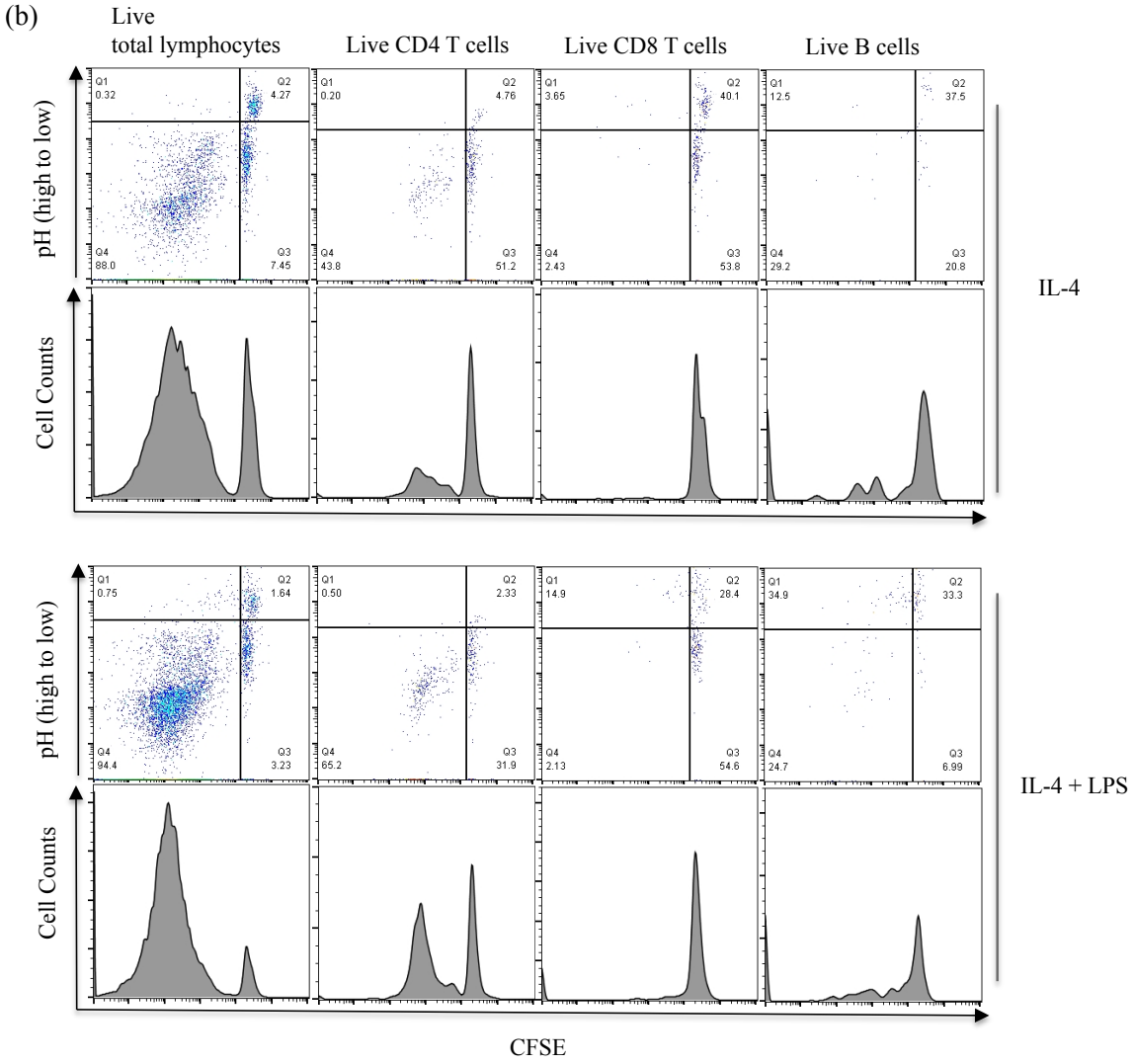

Fig. 1 (b) CFSE-labeled lymph node cells stimulated in vitro with IL-4 or IL-4 and LPS.

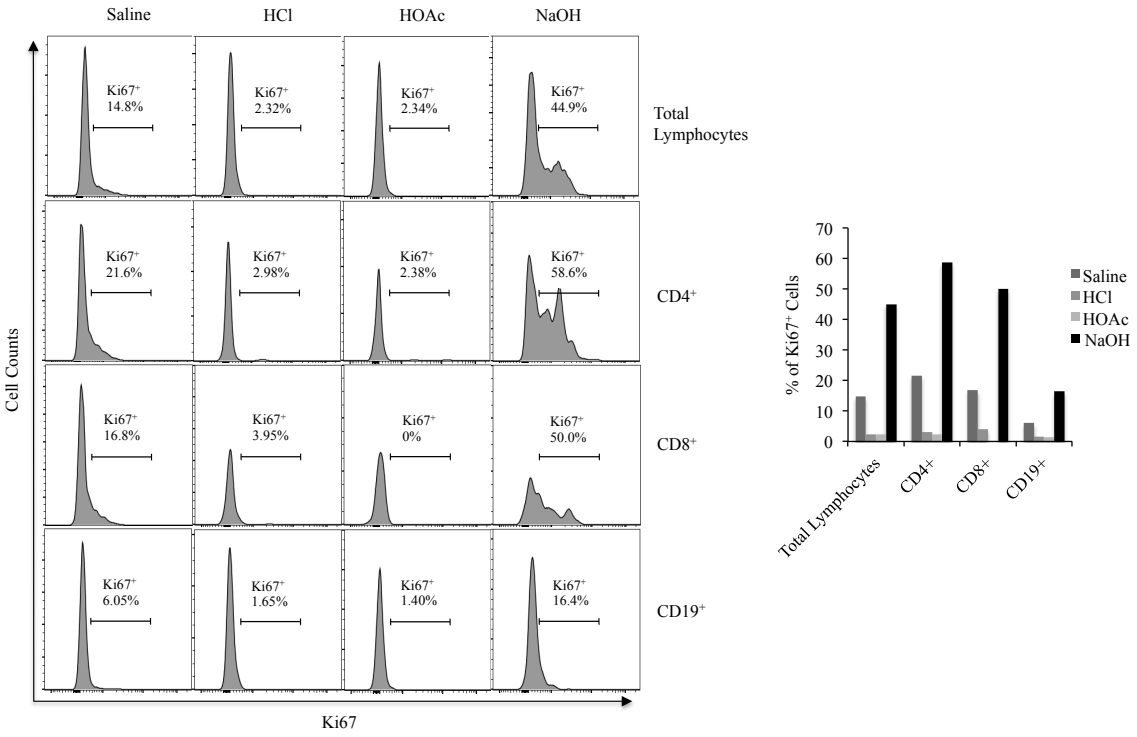

Fig. 2. Effects of in vitro treatments with pH modifiers on lymphocyte proliferation. Primary lymph node cells were incubated in FBS containing 10% saline or saline plus HCl, HOAc or NaOH, then analyzed by flow cytometry to determine Ki-67 expression in live total lymphocytes, CD4, CD8 T cells and B cells ($CD19^+$). Left panels are histograms of Ki-67 expression in the different lymphocyte populations. Right panel is graphic presentation of the percentages of Ki-67^+ cells in the left panels.

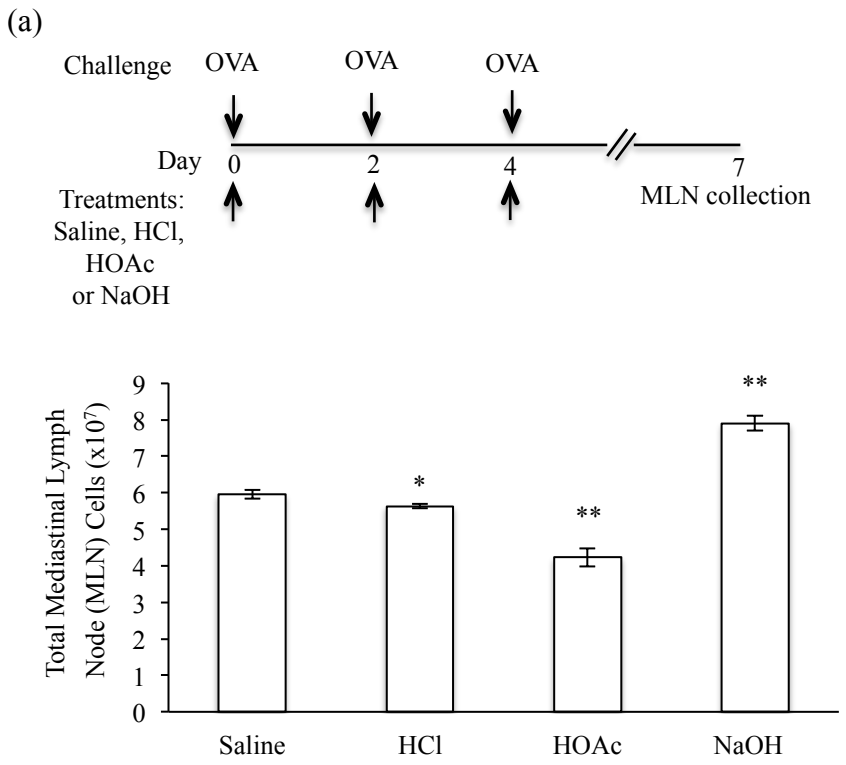

Fig. 3. Effects of in vivo treatments with pH modifiers on the populations and proliferation of lymphocytes in MLNs.

(a) Total numbers of MLN cells. Upper: Schematic illustration of the schedules for OVA challenges and treatments of OVA-sensitized mice with saline, or saline plus HCl, HOAc or NaOH. Arrows indicate the time points for the challenges or treatments. Lower: A graph showing the average total numbers of MLN cells of mice in the different treatment groups. Statistical significance between the saline and the other groups was determined by Student t test; * $p < 0.05$, ** $p < 0.01$.

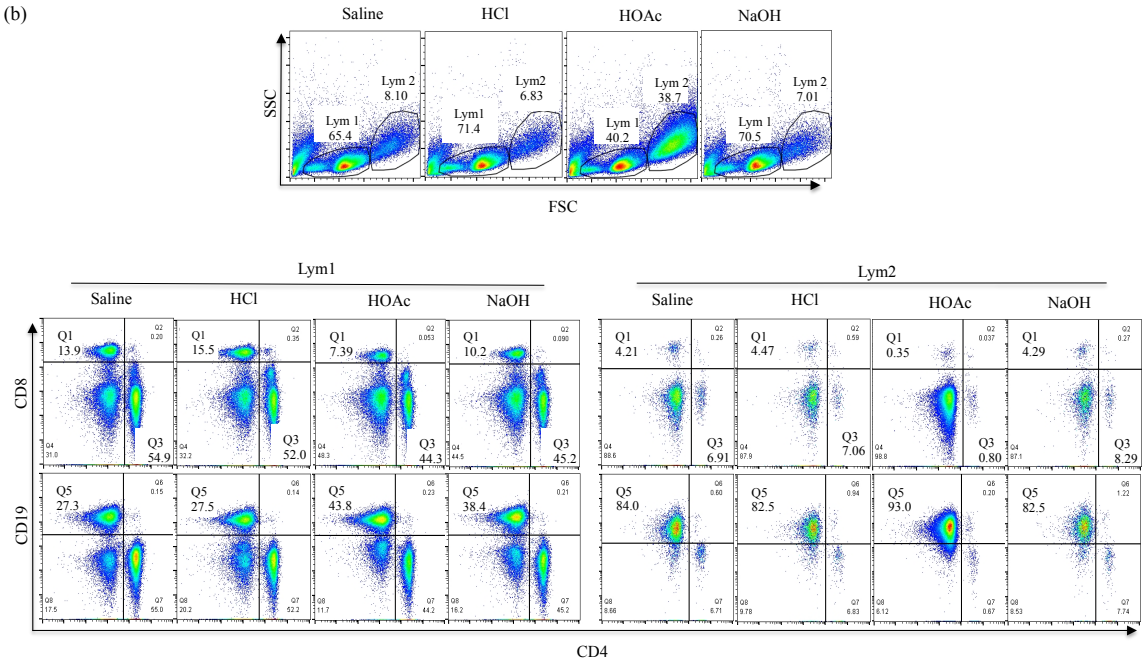

Fig. 3 (b) Lymphocyte populations in the MLNs. The upper panels are flow cytometric plots showing the Lym1 and Lym2 lymphocyte populations in live MLN cells of the different treatment groups. The lower panels show the populations of CD4, CD8 T cells and B cells ($CD19^{+}$) in Lym1 and Lym2. Numbers in the plots are the percentages of each cell populations.

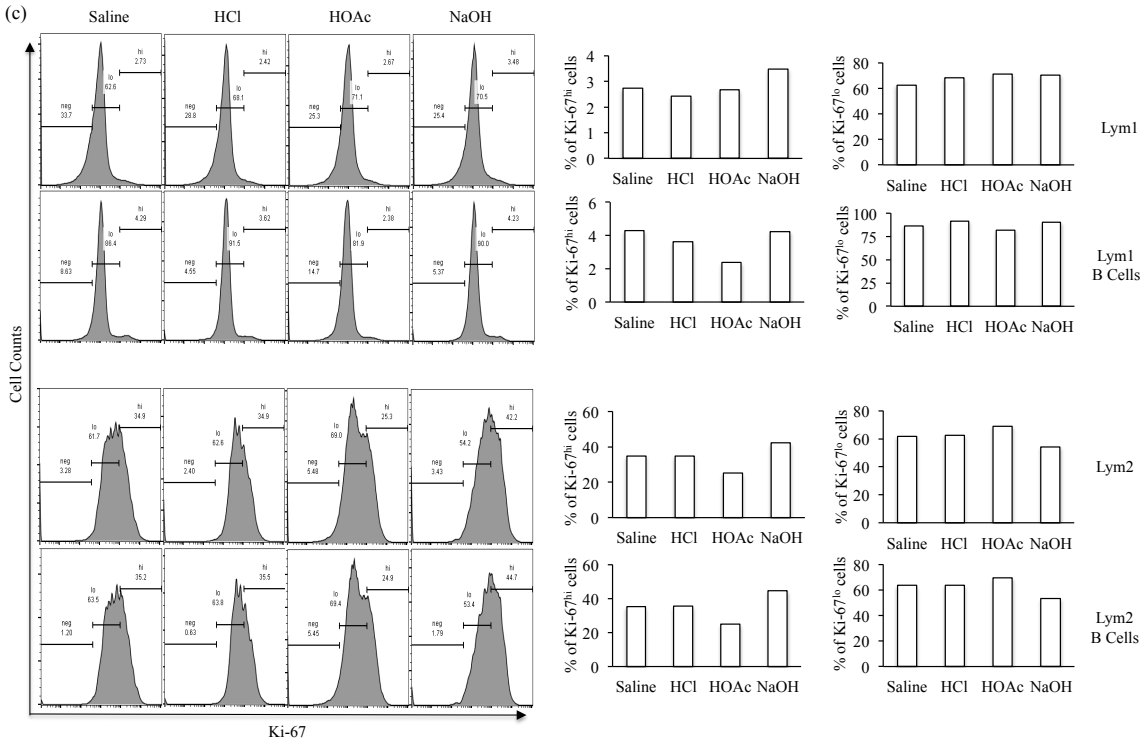

Fig. 3(c) Expression of Ki-67. Left panels are histograms showing Ki-67 expression, and the percentages of Ki-67 high, low, and negative cells in Lym1, Lym2 and B cells thereof. Right panels are graphic presentation of the percentages of the Ki-67 high and low cells in the left panels.

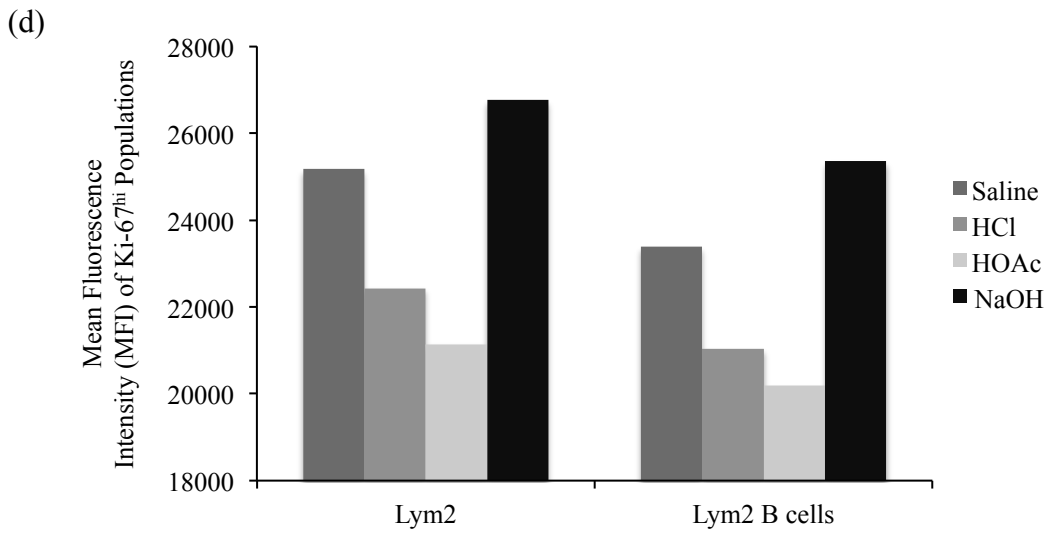

Fig. 3 (d) Mean fluorescence intensities of Ki-67^{hi} cells in the Lym2 populations and their B cells of the different treatment groups.

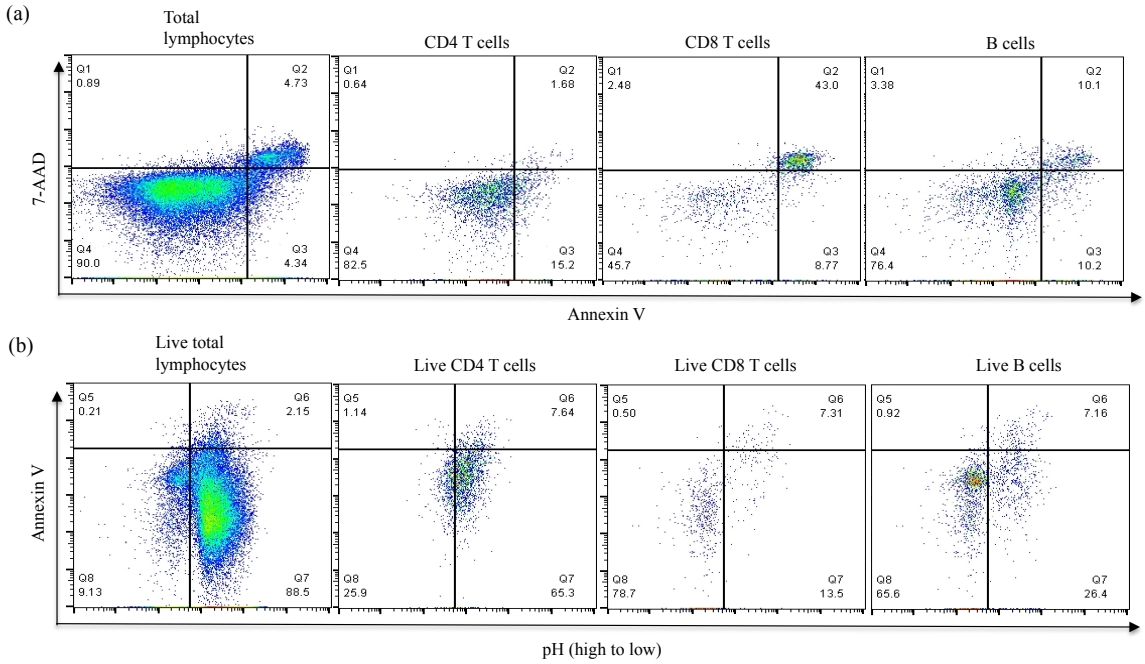

Fig. 4. Relation between low intracellular pH and lymphocyte apoptosis. Total lymphocytes, CD4, CD8 T cells and B cells were analyzed by flow cytometry for the staining of Annexin V, 7AAD or Zombie-violet, and the pH indicator pHrodo^{TM} Green.

(a, b) Steady-state peripheral lymphocytes of unimmunized mice.

(a) Plots showing the staining of Annexin V and 7AAD in the different lymphocyte populations. Apoptotic cells are Annexin V^{hi} 7AAD^{+}, early apoptotic cells are Annexin V^{hi} 7AAD^{-}.

(b) Plots showing the staining of the pH indicator and Annexin V in the live (7AAD^{-}) populations of the different lymphocytes.

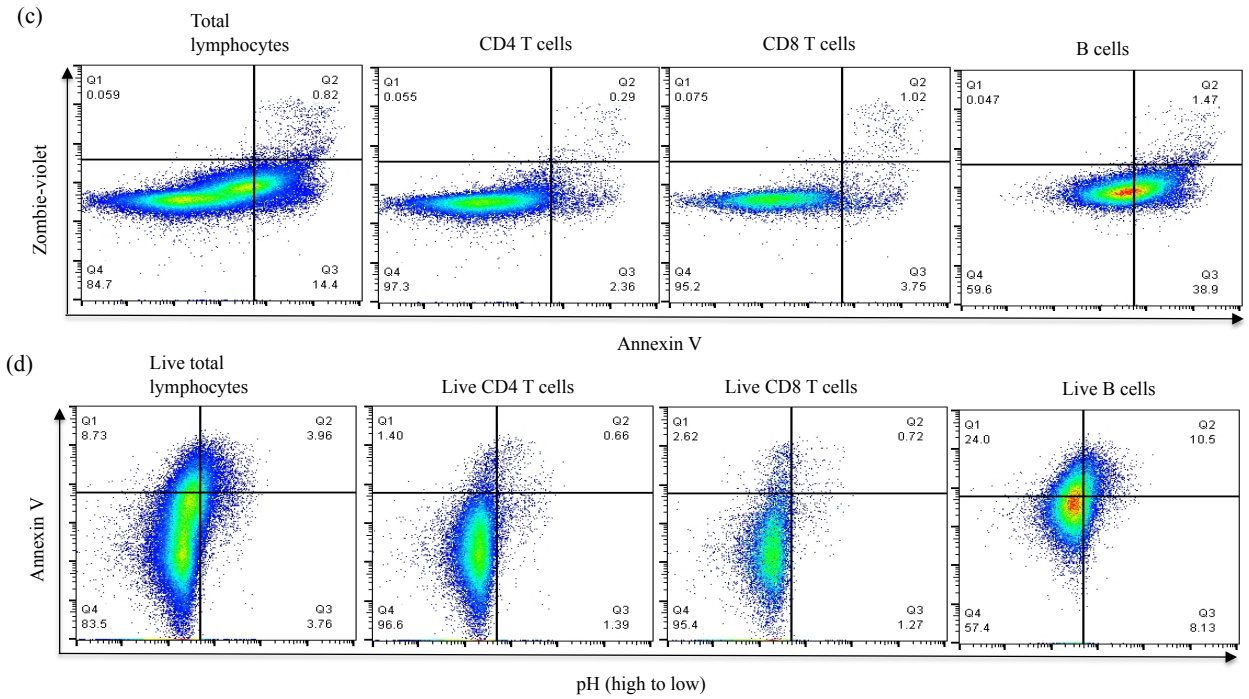

Fig. 4 (c, d, e, f, g) Ex vivo MLN cells of OVA-sensitized and challenged mice.

(c) Plots showing the staining of Annexin V and Zombie-violet of the different lymphocytes.

(d) Plots showing the staining of Annexin V and the pH indicator in the live populations (Zombie-violet $^{lo/-}$) of the different lymphocytes.

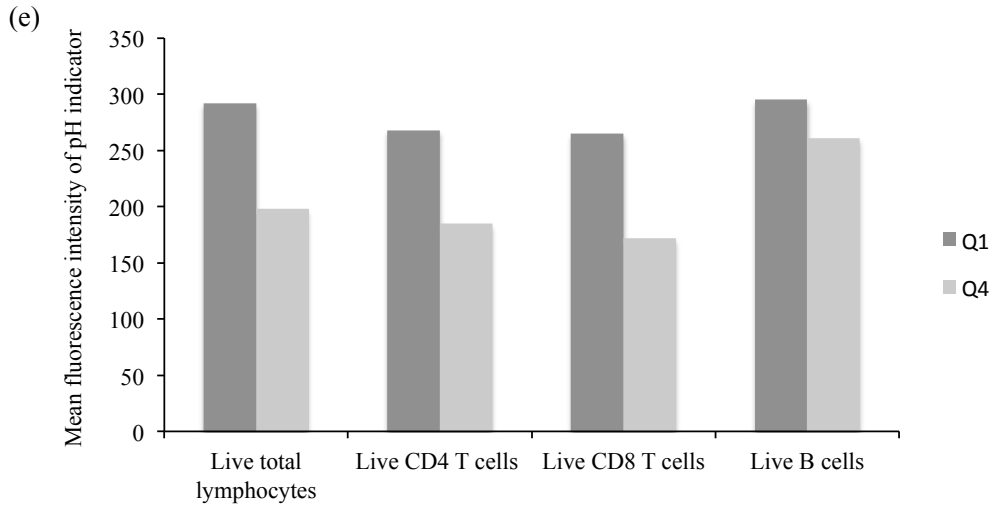

Fig. 4 (e) Bar graphs showing the mean fluorescence intensities (MFI) of the pH indicator staining of the early apoptotic (Annexin V^{hi}) cells in quadrant 1 (Q1) and the non-apoptotic (Annexin V^{lo}) cells in quadrant 4 (Q4) in (d).

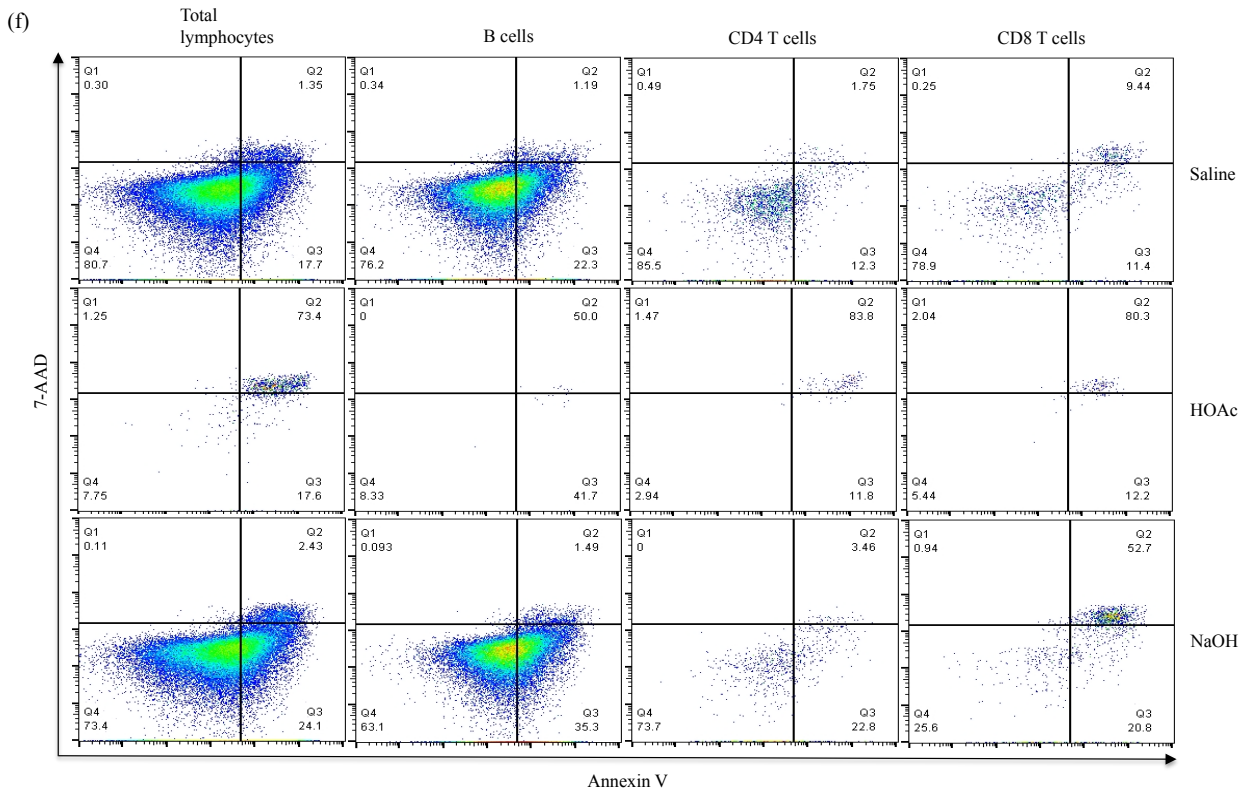

Fig. 4 (f, g). Effects of in vitro treatments with pH modifiers on apoptosis of the MLN lymphocytes. MLN cells from mice that were sensitized and challenged with OVA were treated in vitro with saline or saline plus HOAc or NaOH in FBS.

(f) Plots showing the staining of 7AAD and Annexin V of the different lymphocytes in the different treatment groups.

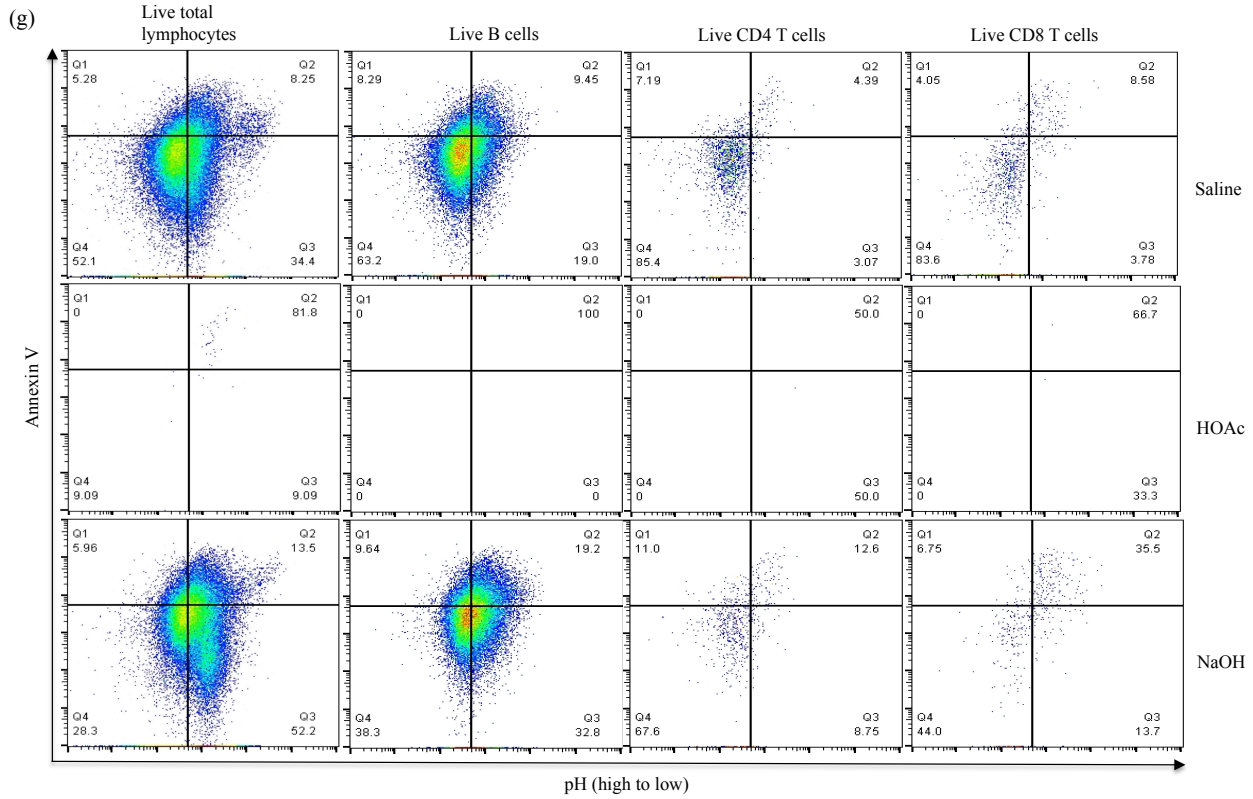

Fig. 4 (g) Plots showing the staining of the pH indicator and Annexin V in the live populations of the different lymphocytes.

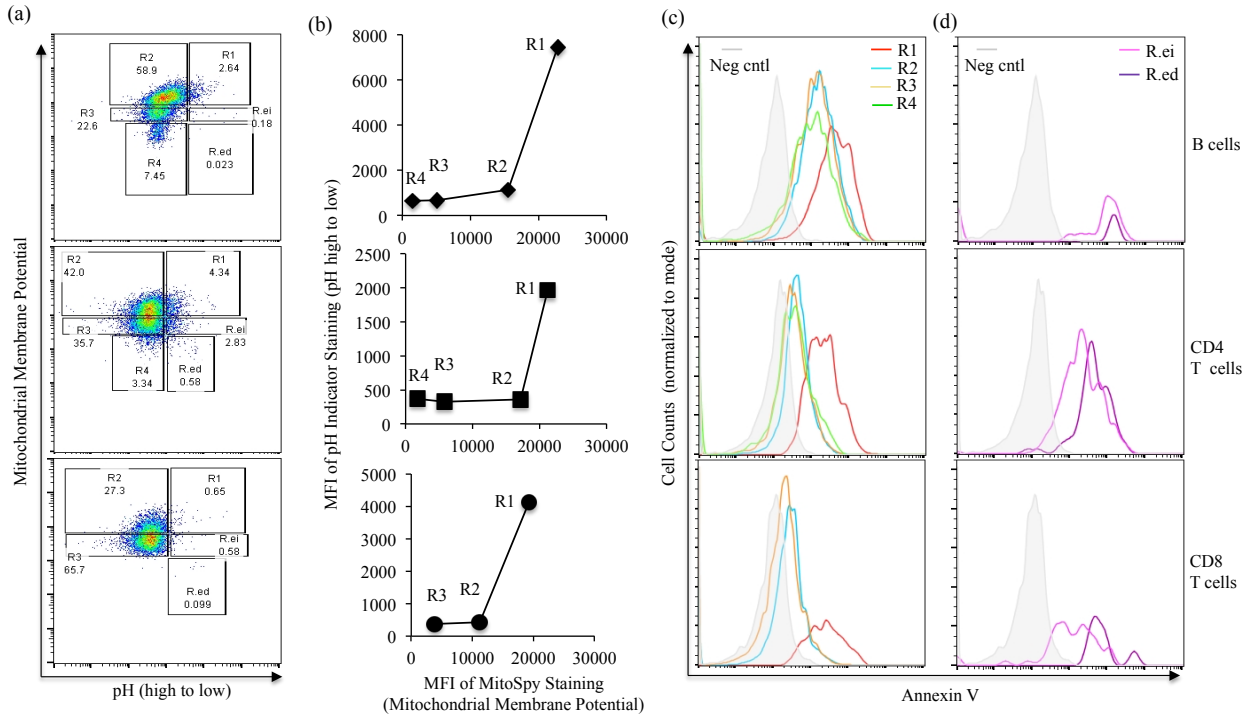

Fig. 5. Relations between mitochondrial membrane potentials and intracellular pH and apoptosis. OVA sensitized mice were challenged with OVA on day 1 and 2, and MLNs were harvested on day 3. MLN cells were stained with MitoSpy and the pH indicator. Flow cytometric analyses of live B cells, CD4 and CD8 T cells are shown.

(a) Pseudocolor plots of MitoSpy and the pH indicator, showing the energy sufficient cell populations (R1 to R4), and energy insufficient (R.ei) and energy deficient (R.ed) populations. Numbers in each gated region are the percentages of cells in the region.

(b) Scatter plots showing intracellular pH (represented by the mean fluorescence intensity (MFI) of the pH indicator staining) as the function of mitochondrial membrane potential (represented by MFI of MitoSpy staining).

(c) Overlaid histograms showing Annexin V staining of the R1 to R4 populations.

(d) Overlaid histograms showing Annexin V staining of the R.ei and R.ed populations

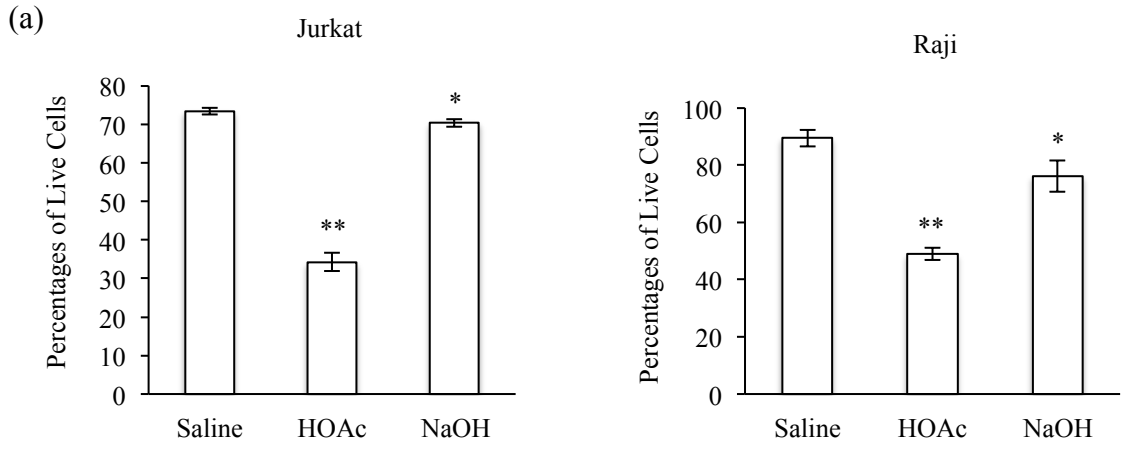

Fig. 6. Effects of pH modifiers on the proliferation and apoptosis of tumor cells.

(a) Comparison of the average viabilities of Jurkat and Raji cells as determined by Trypan Blue staining after treatments with saline or saline plus HOAc or NaOH in FBS. Statistical significance of differences between the saline and other treatment groups was determined by Student t test, * $p < 0.05$, ** $p < 0.01$.

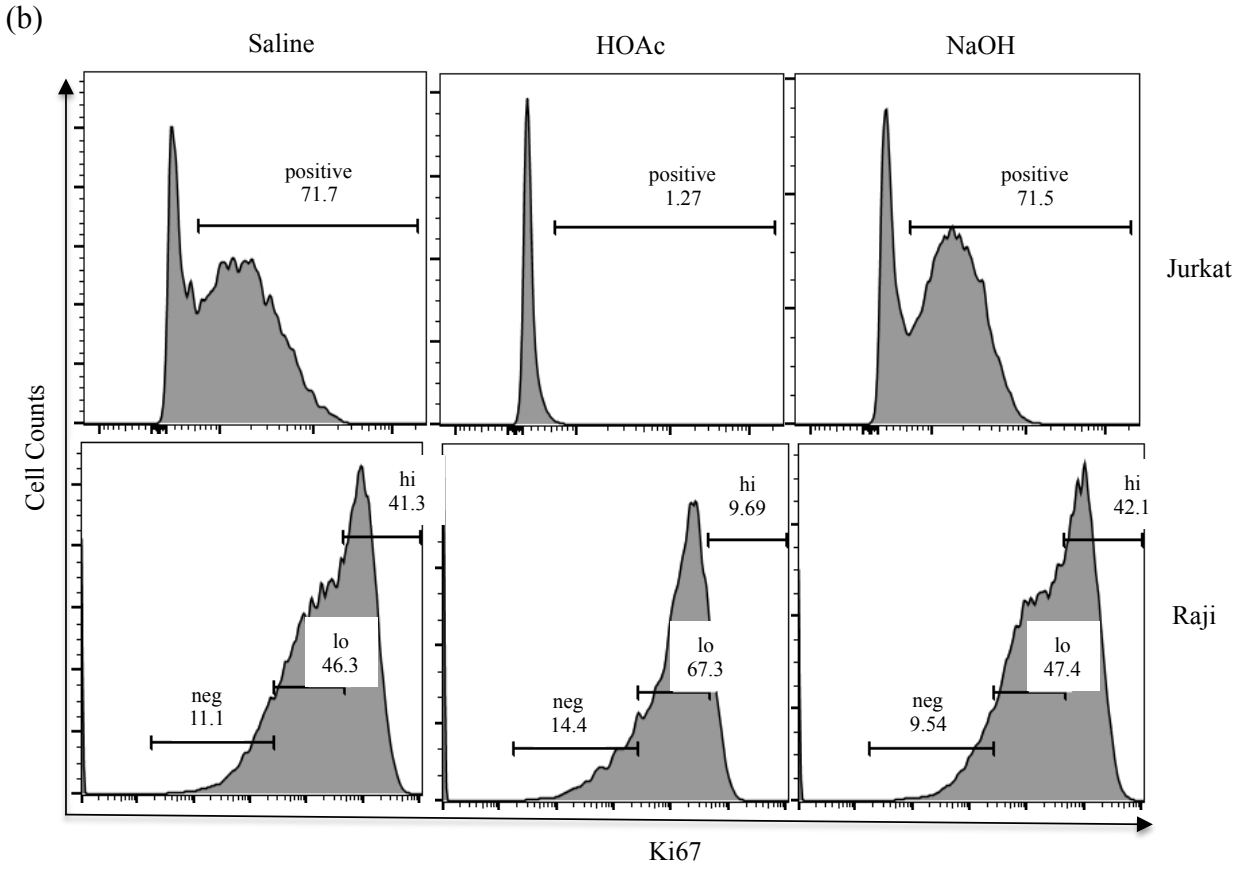

Fig. 6 (b) Histograms of Ki-67 staining in live Jurkat or Raji cells after the different treatments. The numbers in the histograms are the percentages of each population defined by their levels of Ki-67 staining.

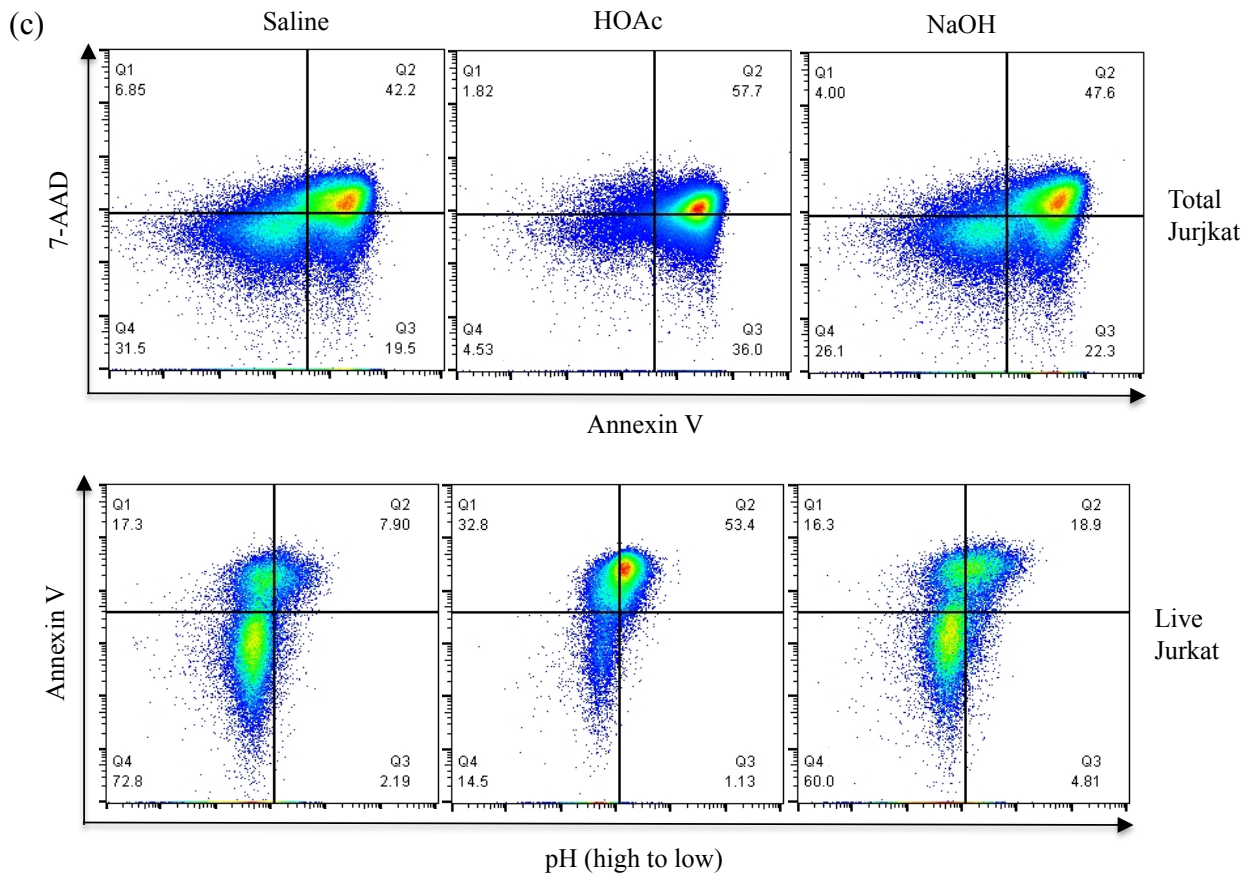

Fig. 6 (c) Apoptosis of Jurkat cells. Upper panels show the staining of 7AAD and Annexin V of Jurkat cells after the different treatments. Lower panels show the staining of the pH indicator and Annexin V in live ($7AAD^-$) Jurkat cells after the treatments.

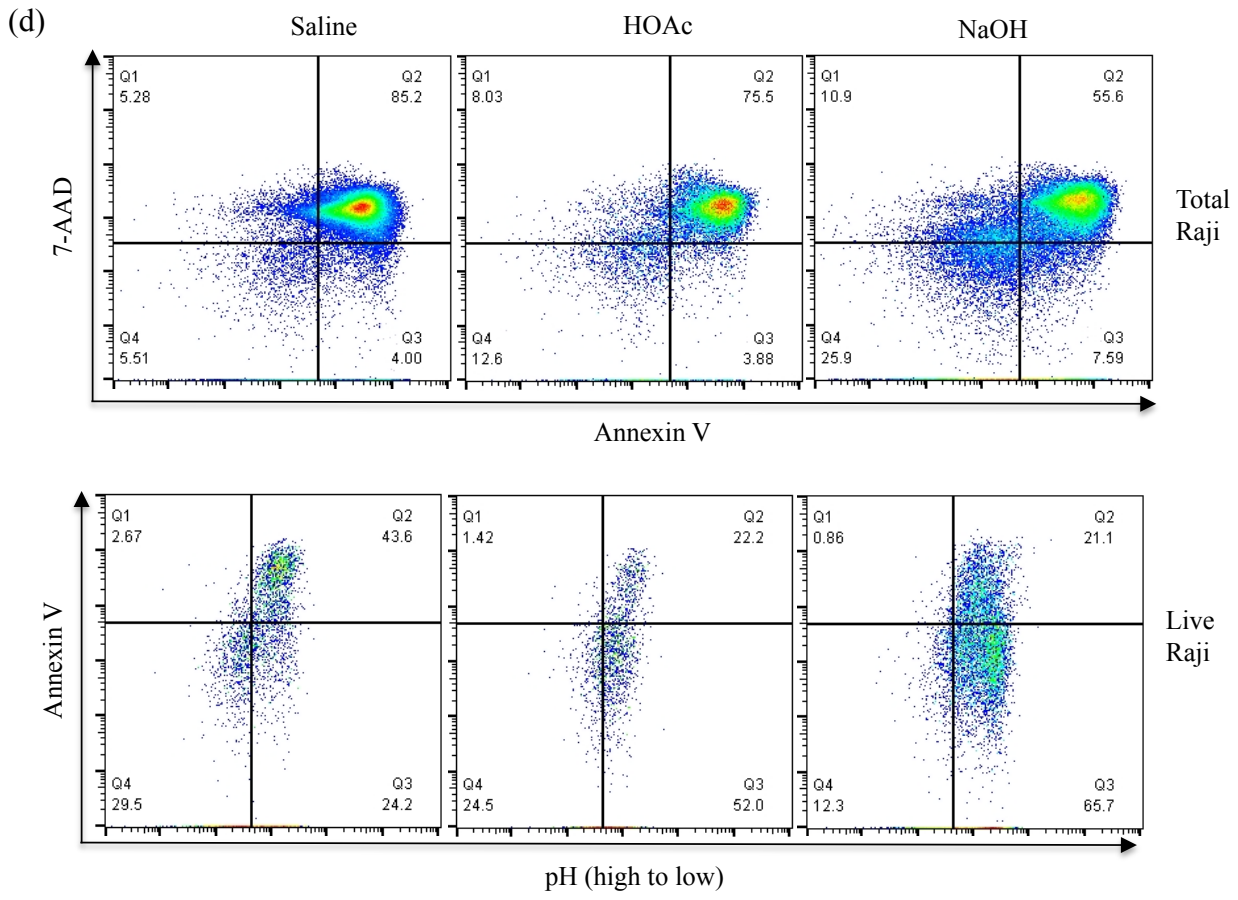

Fig. 6 (d) Apoptosis of Raji cells. Upper panels show the staining of 7AAD and Annexin V of Raji cells after the different treatments. Lower panels show the staining of the pH indicator and Annexin V in live Raji cells after the treatments.

Supplemental Information

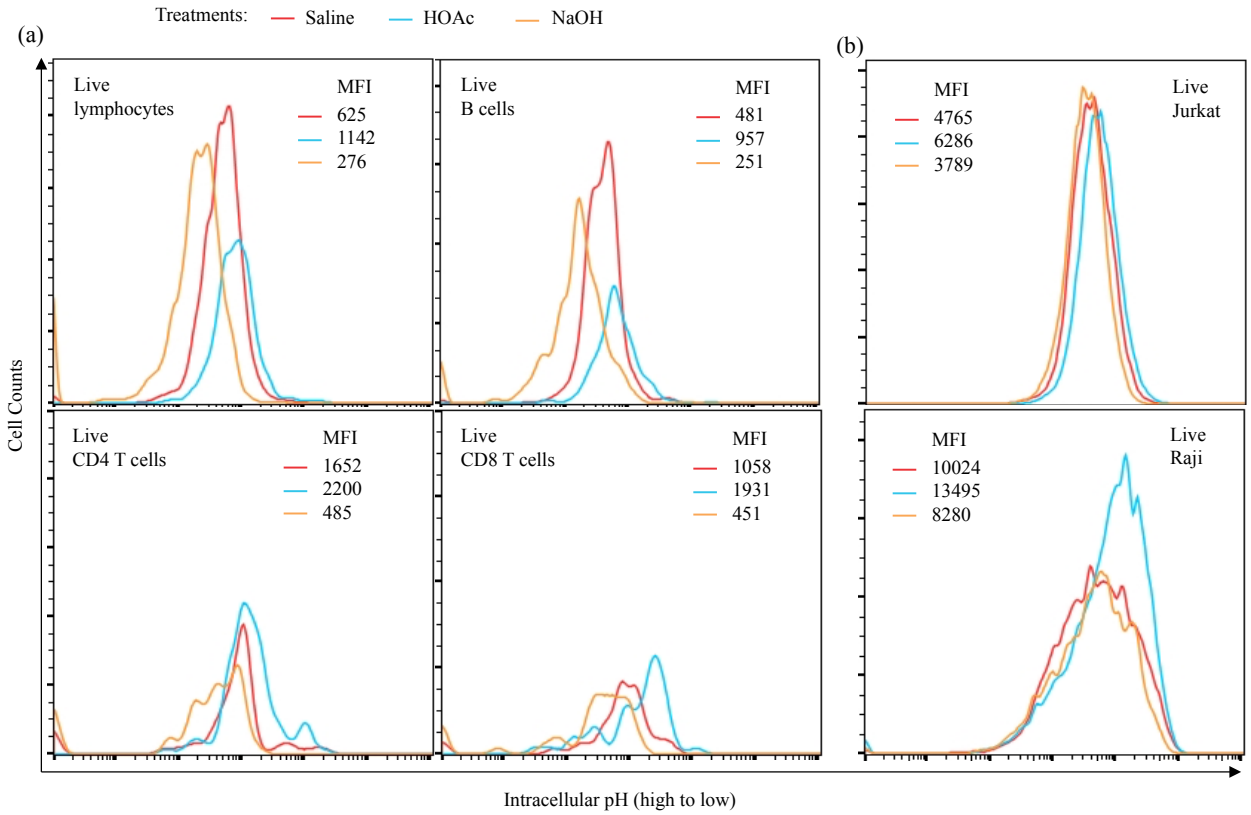

Suppl. Fig. 1. Alteration of intracellular pH by treatments with pH modifiers. Lymphocytes or tumor cells were treated in vitro with saline, or saline plus HOAc or NaOH in FBS. Live cells after the treatments were analyzed for intracellular pH as measured by the staining of the pH indicator pHrodo^{TM} Green. MFI: mean fluorescence intensity of pHrodo^{TM} Green staining.

(a) Overlaid histograms of intracellular pH of different lymphocyte populations of the MLN cells. OVA-sensitized mice were challenged with OVA every other day for a total of 3 challenges. MLNs were harvested on day 9 after the first challenge.

(b). Overlaid of histograms of intracellular pH of Jurkat and Raji cells.

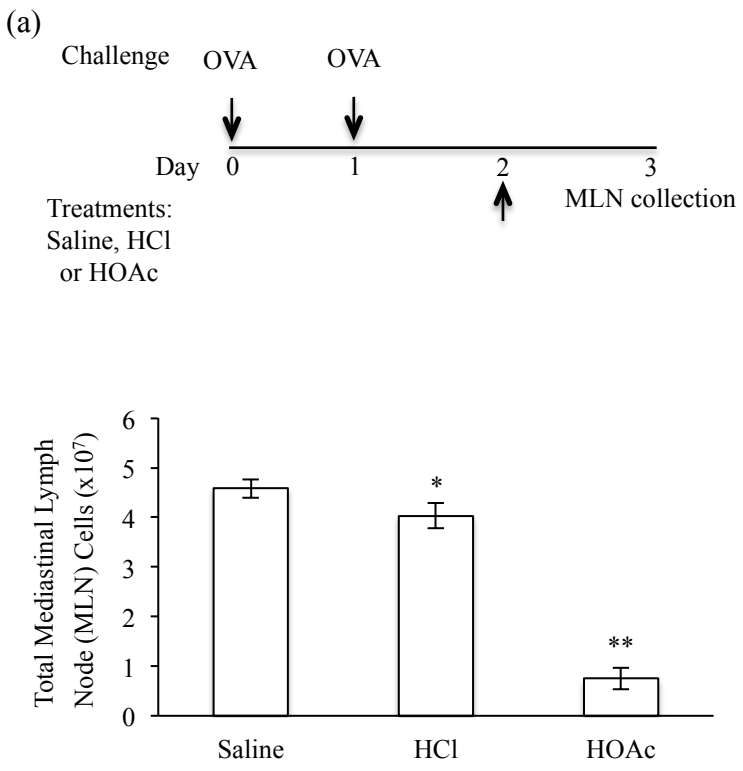

Suppl. Fig. 2. Effects of pH modifiers on the populations and proliferation of lymphocytes in MLNs 3 days after initial OVA challenge.

(a) The top panel is a schematic illustrating the schedules for OVA challenges and treatments with saline, or saline plus HCl or HOAc of OVA-sensitized mice. Arrows indicate the time points of the challenges or treatments. The lower panel shows the average total numbers of MLN cells of mice in the different treatment groups. Statistical significance between saline and the other groups was determined by Student t test; * $p < 0.05$, ** $p < 0.01$.

(b)

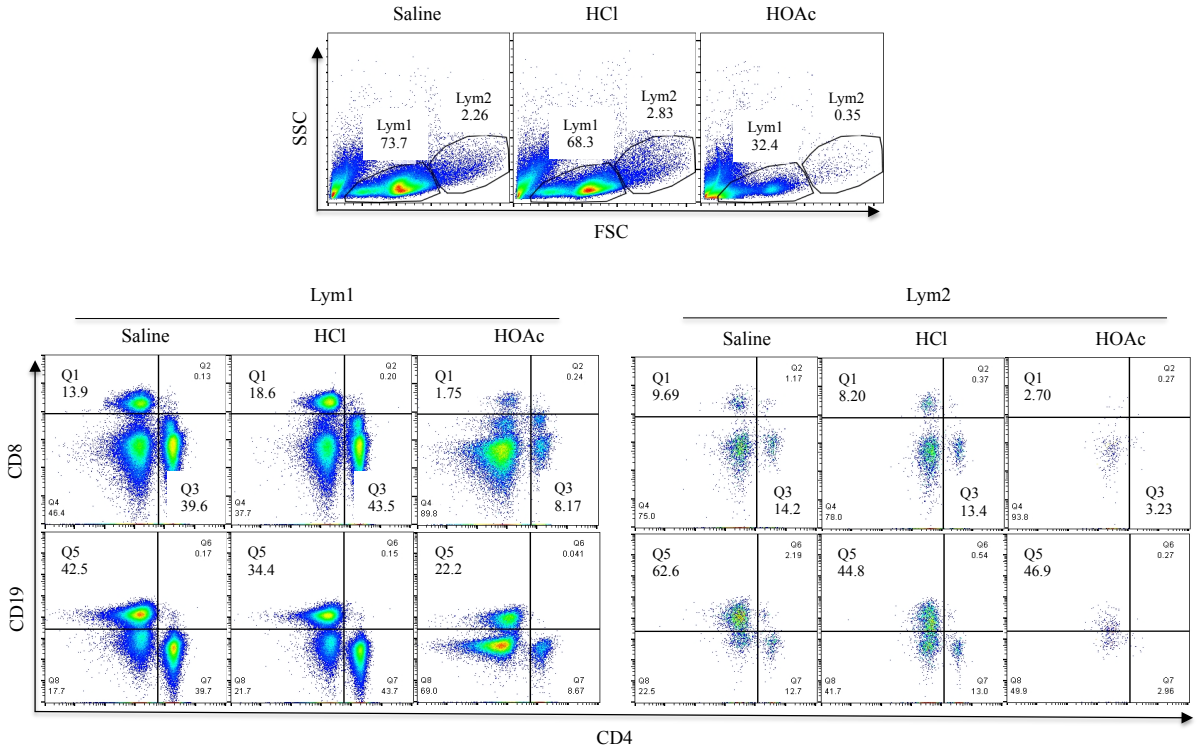

Suppl. Fig. 2 (b) The upper panels show the Lym1 and Lym2 lymphocyte populations in the MLNs of the different treatment groups. The lower panels show the populations of CD4, CD8 T cells and B cells ($CD19^{+}$) in the Lym1 and Lym2 lymphocytes. Numbers in the plots are the percentages of each cell populations.

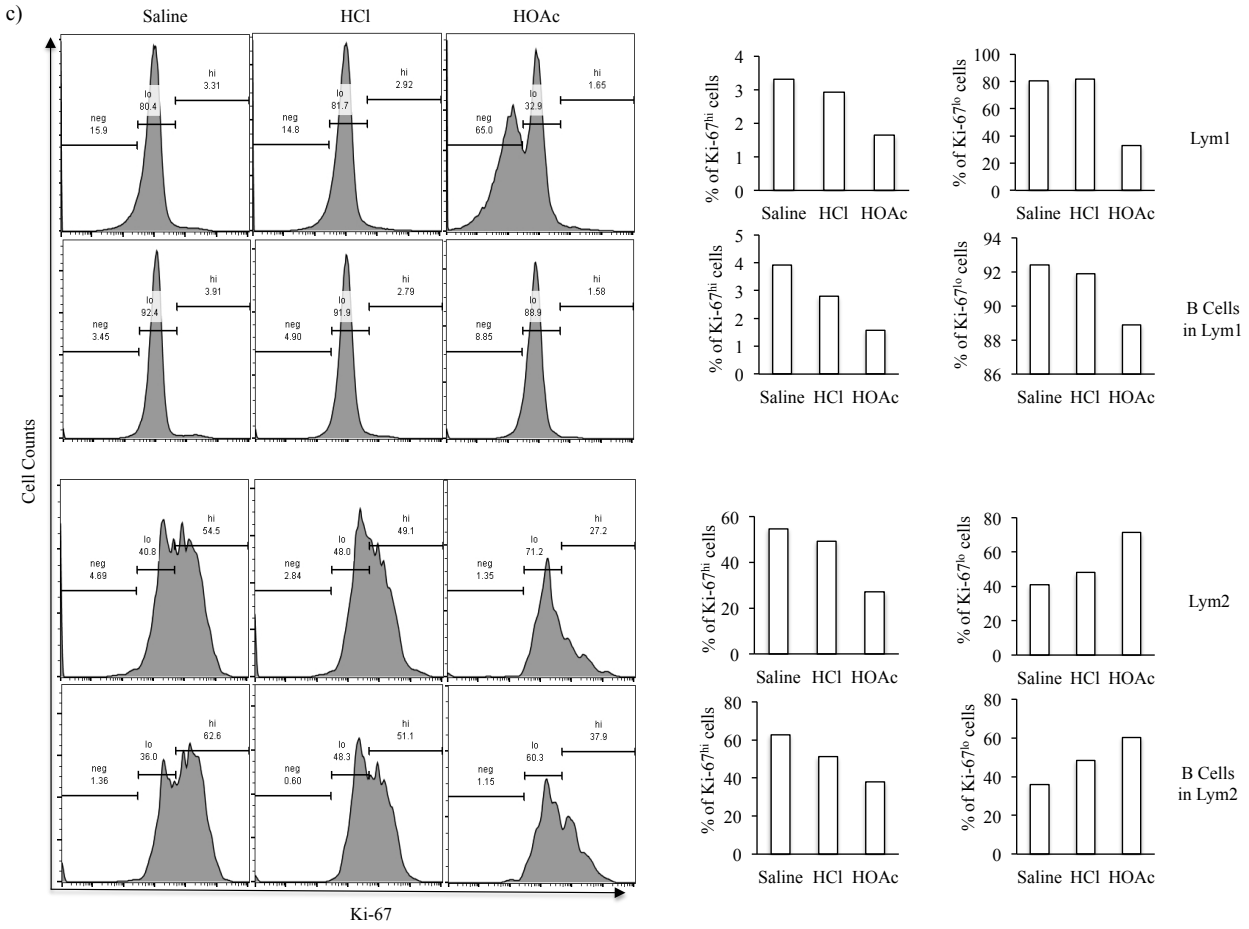

Suppl. Fig. 2 (c) Expression of Ki-67. Left panels are histograms showing Ki-67 expression, and percentages of Ki-67 high, low, and negative cells in Lym1, Lym2 and the B cells thereof. Right panels are graphic presentation of the percentages of the Ki-67 high and low cells.

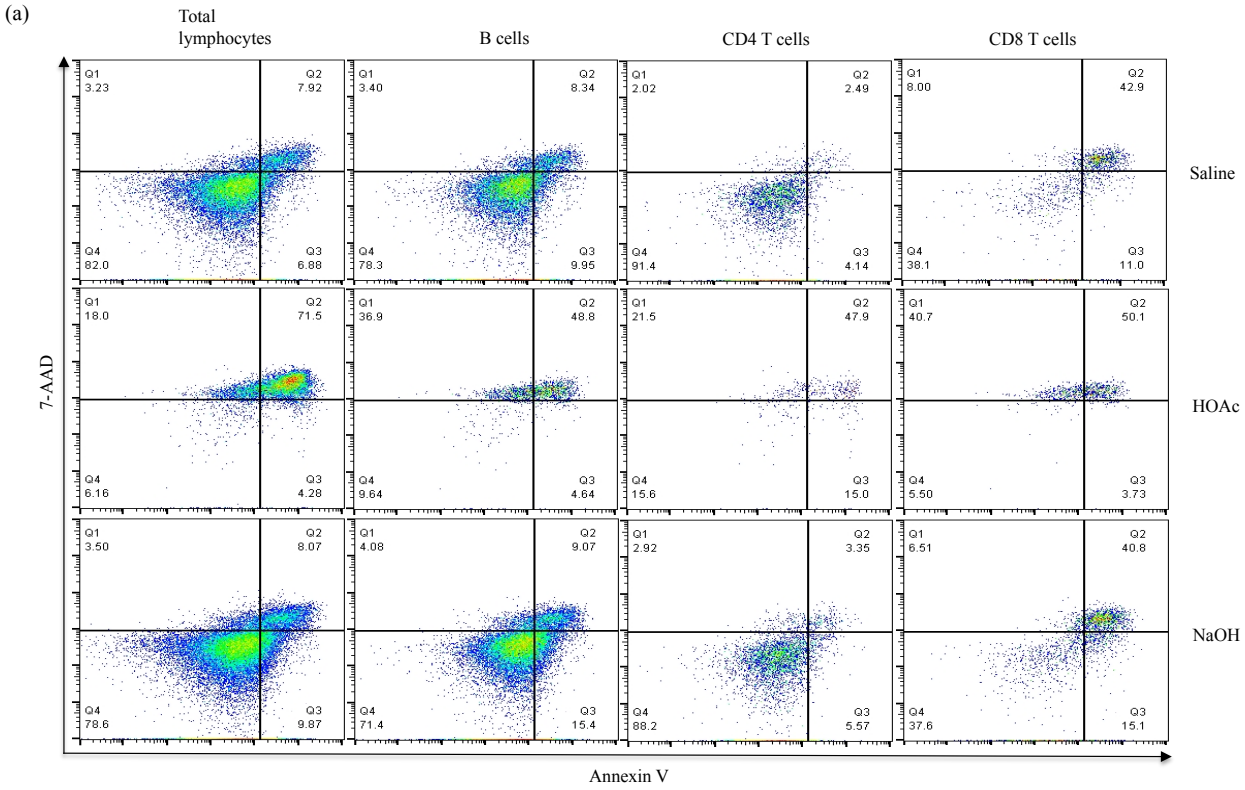

Suppl. Fig. 3. Correlation between low pH and apoptosis of in vitro cultured lymphocytes. After mitogenic stimulation, the cells were treated with saline or saline plus HOAc or NaOH in FBS, then stained with then intracellular pH indicator pHrodo^{TM} Green, Annexin V, and 7-AAD. (a, b) Lymphocytes stimulated with anti-CD3 plus IL-2.

(a) Pseudocolor plots of Annexin V and 7AAD staining of the different lymphocyte populations in the different treatment groups as indicated.

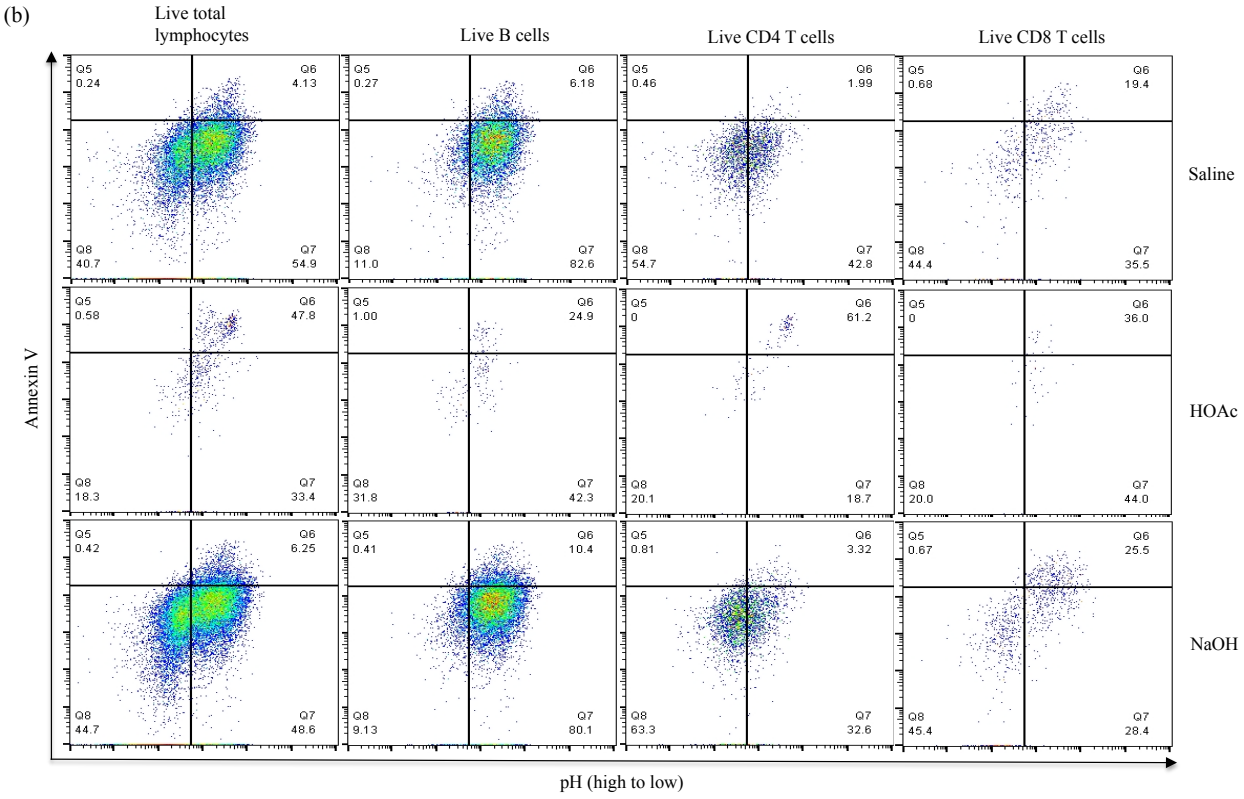

Suppl. Fig. 3 (b) Pseudocolor plots of the pH indicator and Annexin V staining in the different live (7AAD$^-$) lymphocyte populations and treatment groups.

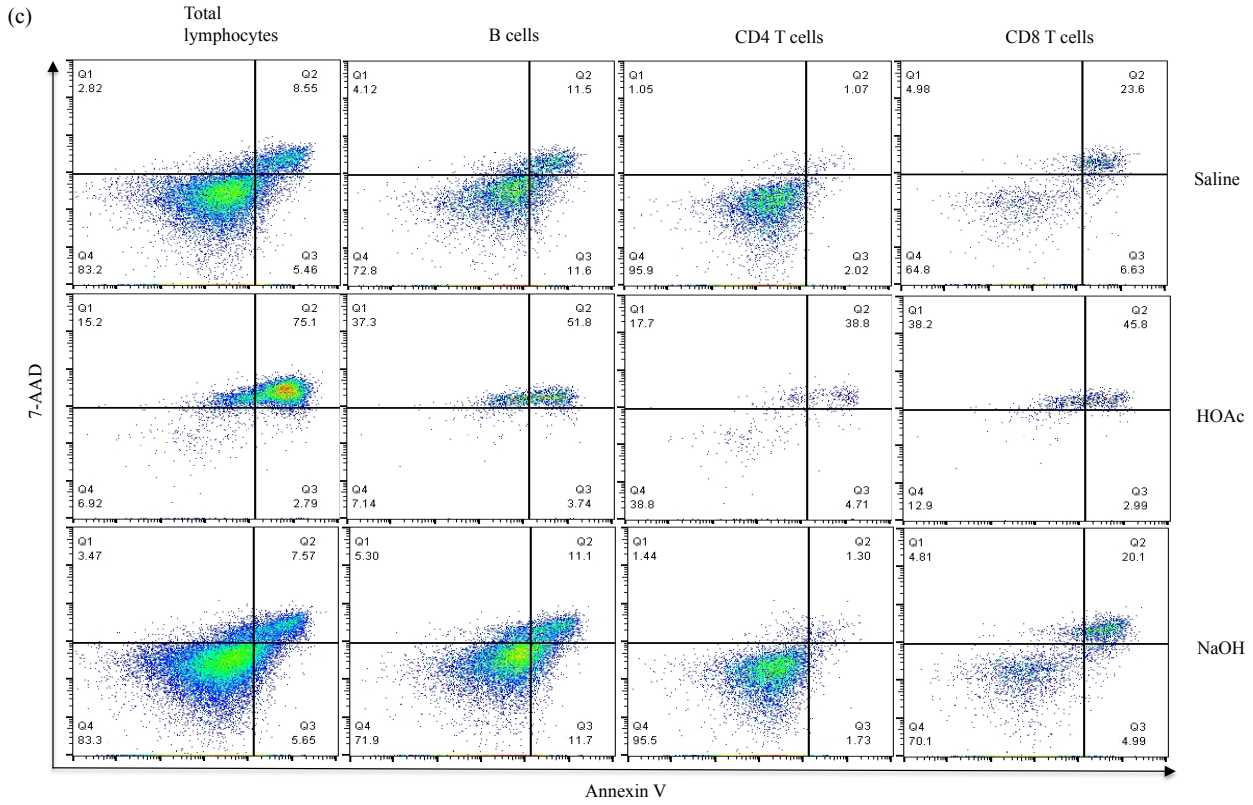

Suppl. Fig. 3 (c, d) Lymphocytes stimulated with LPS plus IL-4.

(c) Plots showing Annexin V and 7AAD staining in the different lymphocyte populations and treatment groups.

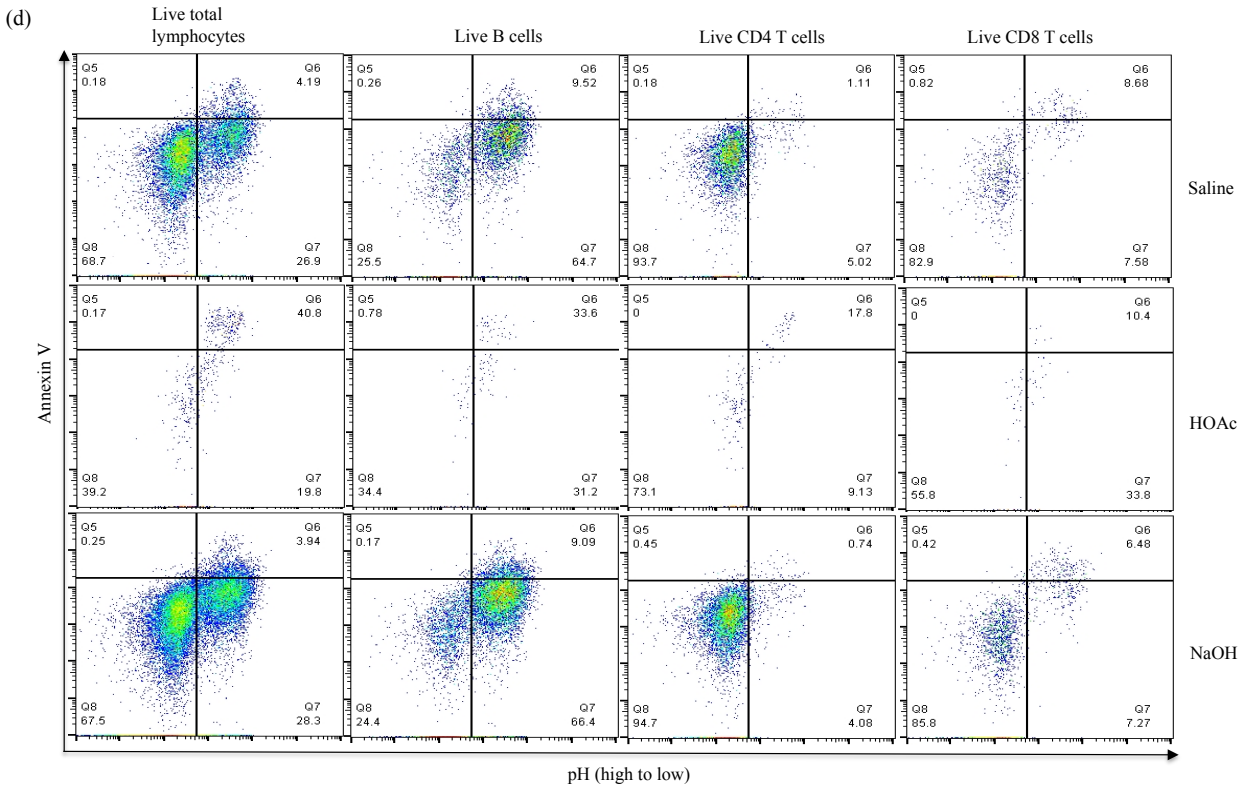

Suppl. Fig. 3 (d) Plots showing the pH indicator and Annexin V staining in the different live (7AAD$^-$) lymphocyte populations and treatment groups.

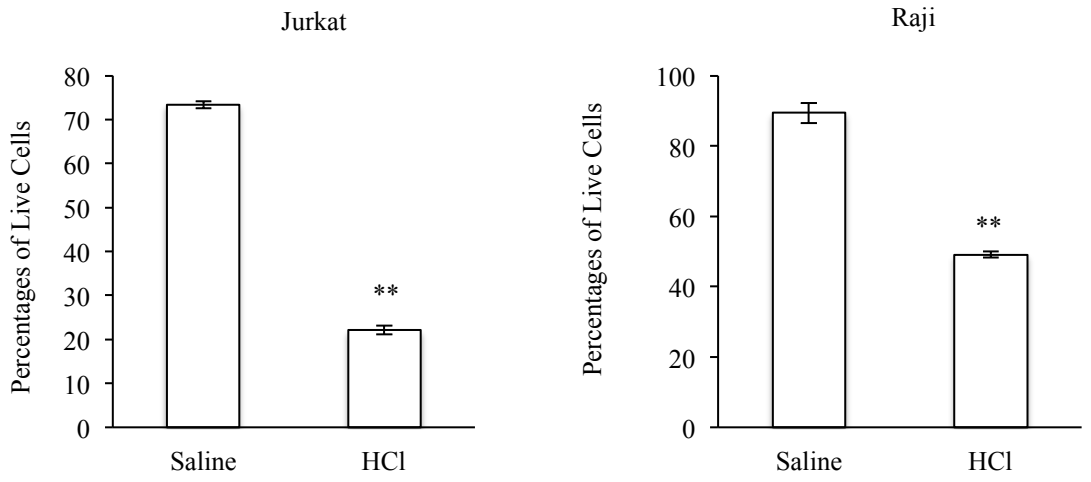

Suppl. Fig. 4. Comparisons of tumor cell viabilities after treatment with saline or saline plus HCl in FBS. Shown are average viabilities of Jurkat and Raji cells determined by Trypan Blue staining in the different treatment groups as indicated. Statistical significance of differences between the saline and HCl treatment groups was determined by Student t test, ** $p < 0.01$.